Modulation of fatty acid elongation sustains sexually dimorphic hydrocarbons and female attractiveness in *Blattella germanica* (L.)

Xiao-Jin Pei [a], Yong-Liang Fan [a, *], Yu Bai [b], Tian-Tian Bai [a], Coby Schal [c], Zhan-Feng Zhang [a], Nan Chen [b], Sheng Li [b], and Tong-Xian Liu [a, *]

[a] State Key Laboratory of Crop Stress Biology for Arid Areas and Key Laboratory of Integrated Pest Management on Crops in Northwestern Loess Plateau, Ministry of Agriculture, Northwest A&F University, Yangling, Shaanxi 712100, P. R. China

[b] Guangdong Provincial Key Laboratory of Insect Developmental Biology and Applied Technology and Institute of Insect Science and Technology, School of Life Sciences, South China Normal University, Guangzhou 510631, China

[c] North Carolina State University, Department of Entomology and Plant Pathology and W.M. Keck Center for Behavioral Biology, Raleigh, North Carolina, USA.

* Corresponding authors:

Y.-L. Fan (yfan@nwafu.edu.cn) and T.-X. Liu (txliu@nwafu.edu.cn).

E-mail addresses:

X.-J. Pei: xiaojinpei@nwafu.edu.cn

Y.-L. Fan: yfan@nwafu.edu.cn

T.-X. Liu: txliu@nwafu.edu.cn

Abstract

Insect cuticular compounds serve multiple functions. As important intersexual signaling chemicals, they show variation between the sexes, but little is known about the underlying molecular mechanisms. Here, we report that sexually dimorphic hydrocarbons (SDHCs) are generated by a fatty acid elongase gene that is regulated by sex-differentiation genes in the German cockroach, *Blattella germanica*. Sexually mature females possess more C29 cuticular hydrocarbons (CHCs), especially the contact sex pheromone precursor 3,11-DimeC29. An RNAi screen and heterologous expression revealed that *BgElo12* and *BgElo24* were involved in HC production, but only *BgElo12* was responsible for SDHCs. Repressing female-enriched *BgElo12* masculinized the female CHC profile, decreased contact sex pheromone level, and reduced the female's sexual attractiveness. Moreover, RNAi of the sex-differentiation genes *BgTra* or *BgDsx* modulated both *BgElo12* transcripts and CHC profiles in females and males. The SDHCs are shaped by sexual selection, as females use them to generate high levels of sex pheromone.

Introduction

Sexual dimorphism is prevalent in the animal kingdom. Females and males independently evolve some traits that enhance survival and reproduction under the pressure of divergent selection forces, thus leading to sexual dimorphism of traits such as body size (Bear and Monteiro, 2013). Under sexual selection, asymmetric selection on the sexes can also result in the evolution of sexually dimorphic traits; however, these traits are subject to both inter- and intra-sexual selection (Darwin, 1871; Andersson, 1994). Because males and females of the same species share the majority of their genomes, the genetic basis of sex-specific traits that evolve under sexual selection is poorly understood. It is widely assumed that sexually dimorphic regulation of gene expression facilitates sex-specific adaptations (Connallon and Knowles, 2005; Innocenti and Morrow, 2010; Mank, 2017; Rogers et al., 2020). Recruitment of pre-existing genes or pathways into sexually dimorphic regulatory contexts has been proposed as a remarkable mechanism enabling the divergence of gene expression between the sexes (Kopp et al., 2012; Williams et al., 2008; Tanaka et al., 2011). The sex-differentiation pathway is a conserved switch or regulator governing a set of downstream genes that direct sexually dimorphic traits (Clough et al., 2014; Prakash and Monteiro, 2016). The signaling cascades that transform sex differences (sex-specific chromosomes) into alternative splicing of sex differentiation genes (e.g. *Transformer* and *Doublesex* in insects), and the patterns of splicing these genes into sex-based isoforms have been widely described in different insect orders (Hasselmann et al., 2008; Zhang et al., 2014a; Kiuchi et al., 2014; Herpin and Schartl, 2015; Hall et al., 2015). However, sexually dimorphic traits are usually generated from tightly associated multiple biosynthetic steps that are executed by a series of genes, and the nodes at which sex-determining signals connect with the biosynthetic pathway are poorly understood. Moreover, how these genes are translated into sexually dimorphic traits under elaborate spatial and temporal patterns also needs to be elucidated.

The main function of insect cuticular hydrocarbons (CHCs) is to waterproof the cuticle to resist dehydration under dry conditions (Gibbs, 1998). In many insects, CHCs have been coopted to serve as chemical signals (pheromones) that mediate intraspecific communication (Blomquist and Ginzel, 2021; Howard and Blomquist, 2005). Sexually dimorphic CHC (SDCHC) profiles are widespread in insects (Ingleby et al., 2014; Zhang et al., 2014b; Berson et al., 2019), but the regulatory networks that underlie the formation of SDCHCs largely remain unknown. Considerable progress has been made toward understanding the genetic basis of HC biosynthesis and CHC variation in insects. An acetyl-CoA

63 carboxylase catalyzes the biosynthesis of malonyl-CoA, and a cytosolic fatty acid synthase (FAS)
64 incorporates malonyl-CoA units onto the acetyl-CoA primer to form linear long-chain fatty acids (LCFAs).
65 A microsomal FAS catalyzes the biosynthesis of methyl-branched LCFAs using methyl malonyl-CoAs
66 (Juárez et al., 1996; 1992; Blomquist et al., 1995; Parvy et al., 2012; Chung et al. 2014; Wicker-Thomas et
67 al. 2015; Ginzel and Blomquist, 2016). The LCF acyl-CoA can be selectively desaturated by a specific fatty
68 acid desaturase (Desat), leading to unsaturated fatty acids (Chertemps et al., 2006; Legendre et al., 2008).
69 The LCF acyl-CoAs are elongated to form very-long-chain fatty acids (VLCFAs) with specific chain
70 lengths by a fatty acid elongation system, including a rate-limiting elongase (ELO) and three other enzymes
71 (Chertemps et al., 2007; Wicker-Thomas et al., 2015). The VLCF acyl-CoAs are finally reduced to long-
72 chain alcohols by fatty acyl-CoA reductases (FARs) and converted to HCs by the P450 oxidative
73 decarbonylase CYP4Gs (Qiu et al., 2012; MacLean et al., 2018; Li et al., 2019a). It is now clear that the
74 variation in CHCs is primarily reflected in the chain length, number and positions of methyl groups, and the
75 degree of unsaturation, which are determined by ELOs, FASs, and Desats, respectively (Blomquist and
76 Bagnères, 2010; Chung and Carroll, 2015; Holze et al., 2020). These genes have been studied in few insect
77 species with regard to SDHCs.
78 In the fruit fly *Drosophila melanogaster*, several studies have elucidated the pheromonal sexual
79 dimorphism of CHCs. Female flies produce C27 and C29 dienes (7,11-heptacosadiene and 7,11-
80 nonacosadiene), both of which function as female-specific contact sex pheromone components, whereas
81 male flies produce C23 and C25 monoenes (7-tricosene and 7-pentacosene) (Ferveur and Sureau, 1996).
82 Ferveur et al. (1997) found that the targeted expression of a sex-differentiation gene, *Transformer*, in male
83 oenocytes feminized the male CHC profile, and elicited homosexual courtship from other males. These
84 findings implicated sex-differentiation genes in the production of SDHCs. About 10 years later, Chertemps
85 et al. (2006) revealed that the female-specific *desatF* was responsible for the generation of pheromonal
86 dienes in female *D. melanogaster*, and they also found that the sexual dimorphism in HC chain length was
87 modulated by the female-specific *eloF* (Chertemps et al., 2007). The specific expression of *desatF* in *D.*
88 *melanogaster* females was due to a special *cis*-regulatory element (CRE) located upstream of *desatF* in *D.*
89 *melanogaster*; the CRE presented a doublesex protein (Dsx) binding site that could be recognized by the
90 female-specific isoform of *Dsx* (*Dsx-F*), and the binding of Dsx-F activated the transcription of *desatF*,
91 whereas male-specific Dsx showed no regulatory activity, resulting in sexual dimorphism of *desatF*

92 expression (Shirangi et al., 2009). However, the regulation of other genes involved in the production of
93 SDHCs remains unknown in *D. melanogaster*, and studies in other insects are even rarer.
94 The German cockroach, *Blattella germanica* is a significant worldwide indoor pest (Schal, 2011).
95 Considerable work has been done on biochemical aspects of CHCs in *B. germanica* (Chase et al., 1990;
96 Juárez et al., 1992; Schal et al., 1994; Juárez, 2004). CHCs in *B. germanica* function as waterproofing
97 agents (Young et al., 2000), and as importantly, specific HC components are also the biosynthetic
98 precursors for the production of contact sex pheromone components. 3,11-DimeC29 is the most abundant
99 CHC in females. Its hydroxylation at the 2 position, catalyzed by an age- and sex-specific putative
100 cytochrome P450 and further oxidation of the -OH generates the main female-specific contact sex
101 pheromone component, 3,11-DimeC29-2-one (Chase et al., 1992). The contact sex pheromone is an
102 efficient courtship signal. When a sexually mature male's antennae detect the sex pheromone on the female
103 body surface (mainly the antennae), a "fencing" of male and female antennae ensues. The male then rotates
104 his body and orients the abdominal tip toward the female's head, while raising his wings to expose a
105 specialized tergal gland. Nutrients in the tergal secretion functions as phagostimulants, placing the female
106 in an appropriate position for copulation while she is engaged in feeding on the secretion (Nojima et al.,
107 1999; Eliyahu et al., 2008a; 2009). More recently, Wexler et al. (2019) decoded the alternative splicing
108 patterns of sex-differentiation genes in *B. germanica*. BgTra is only functional in females and can splice
109 *BgDsx* into two non-functional female-specific isoforms ($BgDsx^F$), whereas males generate a complete
110 functional male-type *BgDsx* ($BgDsx^M$). These findings provide opportunities for exploring the mechanisms
111 underlying the SDHCs in *B. germanica*.
112 In this study, we employed *B. germanica* as a model insect. We characterize the SDCHCs, describe
113 their temporal development, identify *BgElo* genes and provide evidence that *BgElo12* is responsible for the
114 formation of SDCHC profiles. In addition, we found that the female-enriched HCs are important in the
115 generation of the female-specific contact sex pheromone; RNAi of *BgElo12* in females decreased courtship
116 responses of males. Moreover, we show that *BgElo12* is under the regulation of the sex-differentiation
117 pathway; $BgDsx^M$ can specifically repress the transcription of *BgElo12*. These findings suggest that the
118 generation of SDHCs is achieved by placing a fatty acid elongation gene (*BgElo12*) under the regulation of
119 $BgDsx^M$, and linking the sex-differentiation regulatory cascade with the HC biosynthesis pathway, resulting
120 in the asymmetric gene expression and sexually dimorphic HCs in *B. germanica*.

121 # Results

122 ## Sexually dimorphic of cuticular hydrocarbons in *B. germanica*

123 The temporal development of SDCHCs is rarely reported. In order to understand the molecular
124 mechanisms of SDHC generation, we first analyzed the CHC profiles during sexual maturation. The oocytes
125 of female cockroaches mature after eclosion by taking up vitellogenin until ovulation (Schal et al., 1994),
126 and females become sexually receptive and mate 4-5 days before ovulation (Schal and Chiang, 1995). In our
127 study, female cockroaches oviposited late on day 7 or early day 8 (data not shown), therefore AD1–6 (adult
128 days 1-6) adult cockroaches were used for CHC analysis. Different CHC components were identified as
129 previously described (Jurenka et al., 1989). We found no qualitative differences between males and females,
130 but quantitative differences in CHCs became more apparent with adult age (Source data 1). At an early adult
131 stage (AD1 and AD2), females and males had similar CHC profiles. However, differences were apparent at
132 AD3 and gradually increased until AD6 (Figure 1A). Along with sexual maturation in males, the proportions
133 of C27 CHCs and 9-; 11-; 13-; 15-MeC29 (male-enriched peak 17) obviously increased, while other C29
134 CHCs, particularly 3,7-; 3,9-; 3,11-DimeC29 (female-enriched peak 24) significantly decreased. In females,
135 however, the CHC profiles consistently displayed high proportions of C29 CHCs and especially 3,7-; 3,9-;
136 3,11-DimeC29 (Figure 1B–E). Principal component analysis (PCA) showed that the male and female CHC
137 profiles were more similar at AD1, but diverged at AD6, and the divergence was mainly reflected in principal
138 component 2 which largely represents the chain length factor (Figure 1F–G). The sexual dimorphism of
139 CHCs was generated at the adult stage (nymphal CHC chromatogram showed no qualitative differences
140 between males and females, Figure 1–figure supplement 1), and the sexes diverged with sexual maturation.
141 Notably, the differences between male and female CHC profiles suggested that chain length is an important
142 factor in sexual dimorphism of CHCs.

143

144 ## *BgElo12* and *BgElo24* are involved in HC biosynthesis

145 The genetic basis of HC production in *B. germanica* is not completely understood. Our previous work
146 identified a fatty acid synthase gene (*BgFas1*) and a P450 oxidative decarbonylase gene (*CYP4G19*) that are
147 involved in HC biosynthesis, but both showed no function in the sexual dimorphism of CHCs (Pei et al.,
148 2019; Chen et al., 2020). In this study, we found that the differences of CHCs between females and males

149 are largely reflected in carbon chain length, which suggests that elongase genes may be the crucial regulator
150 of SDCHCs. This was consistent with specific C29 CHCs reported to be enriched in females, and C27 CHCs
151 enriched in males (Wexler et al., 2019). Based on this assumption, we searched for potential *BgElo* genes in
152 the *B. germanica* genomic data and our full length transcriptomic data (Harrison et al., 2018; Pei et al., 2019).
153 A total of 24 different *BgElo* candidate genes were identified, and all *BgElos* were cloned and re-sequenced.
154 Sequence alignment revealed that different BgElo proteins showed high homology and contained the
155 conserved HXXHH and YXYY motifs (Moon et al., 2001). All BgElo proteins displayed a ELO domain and
156 several transmembrane domains (Supplementary file 1).

157 The fatty acid precursors used for HC production generally originate in the oenocytes, but also can be
158 transported from the fat body to oenocytes (Wicker-Thomas et al., 2015). Therefore, we first analyzed the
159 transcript levels of all *BgElos* in the fat body and abdominal integument. Results showed that *BgElo24* and
160 *BgElo12* were highly expressed in the integument, and *BgElo1*, *2*, *3*, *6*, *7*, *9*, *10*, *11*, *14*, *17*, *20*, and *22* were
161 also abundant in the integument, while other *BgElos* were nearly undetectable (Figure 2A). In the fat body,
162 *BgElo10* and *BgElo22* were highly expressed, *BgElo1*, *2*, *3*, *11*, *12*, and *24* were slightly expressed, and other
163 *BgElos* were undetectable (Figure 2B).

164 Based on these results, RNAi of the genes that were expressed in the abdominal integument or fat body
165 was performed. A first injection of dsRNA was performed in early fifth-instar nymphs (N5D1 or N5D2), and
166 a boost injection was performed one week later, and then the treated cockroaches were collected at different
167 adult stages and subjected to CHC analysis. RNAi of different *BgElo* genes significantly decreased the
168 mRNA level (Figure 2–figure supplement 1). GC–MS analysis of CHCs showed that C27 CHCs were
169 affected by many genes – knockdown of *BgElo1*, *10*, *12*, *14*, *20*, and *24* caused a significant increase in C27
170 CHCs, and repression of *BgElo12* showed the greatest increase of the content of C27 CHCs (Figure 2C). C28
171 CHCs were rarely affected, with only knockdown of *BgElo24* causing a significant decrease in C28 CHCs
172 (Figure 2D). C29 CHCs were the most abundant in *B. germanica*, and only RNAi of *BgElo12* or *BgElo24*
173 significantly decreased their amount (Figure 2E). RNAi of *BgElo12* or *BgElo24* also dramatically decreased
174 the amount of C30 CHCs, while RNAi of *BgElo2* increased C30 CHCs (Figure 2F). CHCs with chain lengths
175 greater than 30 occur in low quantities in *B. germanica*, but the most striking result was a sharp decline that
176 resulted from *BgElo24*-RNAi (Figure 2–figure supplement 2). The detailed changes of individual CHCs after
177 RNAi of *BgElos* are available in Source data 2. In conclusion, these data strongly suggest that *BgElo12* and

178 *BgElo24* are involved in CHC production, but we cannot rule out that other *BgElo* genes might have a less
179 prominent role in HC biosynthesis.
180

181 **_BgElo12_ is the terminal gene in maintaining sexually dimorphic hydrocarbon profiles**

182 Although, it appears that both *BgElo12* and *BgElo24* are involved in HC production, it is unclear which
183 gene is responsible for sexual dimorphism of CHCs. Therefore, we compared the CHC profiles of treated
184 female cockroaches with wild type male cockroaches. The results showed that only RNAi of *BgElo12* made
185 the female CHC profile more similar to the male profile (Figure 3A), reflected by a significant increase of
186 C27 CHCs without affecting the male-enriched peak 17, and a selective downregulation of C29 CHCs, with
187 a dramatic downregulation of the female-enriched peak 24 and some other C29 CHCs (Figure 3B). Also,
188 knockdown of *BgElo12* increased the proportions of C27 CHCs and peak 17, while the proportions of C29
189 CHCs and peak 24 significantly decreased (Figure 3D). These changes converged the female CHC profile
190 toward the male CHC profile. The repression of *BgElo24* downregulated all C28–C32 CHCs (Figure 3C),
191 even though knockdown of *BgElo24* increased the proportion of C27 CHCs, and decreased the proportion of
192 C29 CHCs and peak 24 (Figure 3E); the amount of the male-enriched peak 17 was also dramatically
193 downregulated (Figure 3C). Similar results were generated in males, and RNAi of *BgElo12* generated the
194 characteristics of male CHC profiles, while *BgElo24*-RNAi downregulated all C28–C32 CHCs (Figure 3–
195 figure supplement1). In order to confirm these results, a second RNAi target was used for both genes, and
196 similar results were generated (Figure 3–figure supplement 2A–B). In addition, we analyzed the internal HCs
197 after repression of *BgElo12* or *BgElo24*. The internal HCs underwent similar changes as CHCs (Figure 3–
198 figure supplement 2C–D). These results suggest that the changes imposed by *BgElo12*- or *BgElo24*-RNAi
199 were caused by a deficiency in *de novo* HC biosynthesis and not the transport of HCs from internal tissues
200 to the cuticle.

201 We also examined the spatio-temporal expression of *BgElo12* and *BgElo24*. Both *BgElo12* and *BgElo*
202 *24* were primarily expressed in the abdominal integument, where the oenocytes that produce HCs are located
203 (Figure 3–figure supplement 3). Monitoring of *BgElo12* expression in females and males across different
204 developmental stages showed that female and male *BgElo12* mRNA levels were similar at N6D4 and early
205 adult stage, but its expression level was higher in females than in males at AD3, and the difference increased
206 through AD6 (Figure 3F), a pattern similar to the production of SDCHCs. The expression levels of *BgElo24*

207 were higher in males than in females starting at AD2 (Figure 3G). These results also support that only
208 *BgElo12*, and not *BgElo24*, is involved in sexual dimorphism of CHCs in *B. germanica*.
209 Finally, because CHCs are important waterproofing agents in insects (Gibbs, 1998), we investigated the
210 roles of *BgElo12* and *BgElo24* in desiccation resistance. We found that repression of *BgElo24* dramatically
211 decreased tolerance of desiccation, but RNAi of *BgElo12* had little effect on desiccation tolerance (Figure
212 3H). These results indicate that the biological significance of *BgElo12* in cockroaches is to support sexual
213 dimorphism of CHCs, whereas *BgElo24* supports desiccation tolerance.
214

215 **BgElo24 provides VLCFA substrates for BgElo12**

216 Thus far, we showed that both *BgElo12* and *BgElo24* are involved in HC production, RNAi of *BgElo12*
217 only selectively decreased some HCs while repression of *BgElo24* dramatically downregulated all C28–C29
218 HCs, and some HCs were affected by both *BgElo12* and *BgElo24*. We also found that knockdown of *BgElo24*
219 caused a two-fold upregulation of *BgElo12*, while RNAi of *BgElo12* had no significant influence on *BgElo24*
220 mRNA level (Figure 4–figure supplement 1A–B). Therefore, we considered whether BgElo24 is a basic
221 elongase that provides substrates used for HC biosynthesis, and if BgElo24 generates primary precursors that
222 can be further catalyzed by BgElo12. We verified the functions of BgElo12 and BgElo24 in VLCFA
223 biosynthesis with heterologous expression of *BgElo12* and *BgElo24* in *Saccharomyces cerevisiae* (strain
224 INVSc1). The genetic background of *S. cerevisiae* is relatively clear, as wild type *S. cerevisiae* contains three
225 different ELO proteins: ELO1 is able to elongate C14 FAs to C16 FAs, ELO2 can generate C24 FAs, and
226 ELO3 plays essential roles in the conversion of C24 FAs to C26 FAs (Toke and Martin, 1996; Oh et al.,
227 1997). In our study, activation of GAL1 promoter by galactose successfully transcribed the target genes, and
228 we detected the expression GFP protein (Figure 4–figure supplement 1C–E). GC–MS analysis of FAs in *S.*
229 *cerevisiae* that contained pYES2-GFP (control) detected large amounts of C16:1, C16:0, C18:1, and C18:0
230 FAs, minor amounts of C20–C24 and C28 FAs, and a larger amount of C26:0 FAs (Source data 3). Yeast
231 with exogenous *BgElo12* did not produce any new FAs, but heterologous expression of *BgElo24* sharply
232 increased the amount of C28:0 FA, and generated a new component, C30:0 FA (Figure 4A–C; Figure 4–
233 figure supplement 1H–I). These results suggest that BgElo24 is capable of elongating endogenous yeast FAs
234 to generate C28:0 and C30:0 FAs.
235 Considering that BgElo12 and BgElo24 may selectively elongate substrates with specific carbon chain

236 lengths, we separately added C20:0, C22:0, C24:0, C26:0, and C28:0 FAs to the medium. Compared with
237 the control, BgElo24 did not produce any new FAs when C20:0, C22:0, C24:0, or C26:0 were added (Source
238 data 3). However, when C28:0 FA was added, yeast with pYES2-BgElo12 generated C30:0 FA, although in
239 small amounts (Figure 4A'–C'; Source data 3). These results suggest that BgElo24 not only directly provides
240 substrates (C28 and C30 fatty acyl-CoAs) for the biosynthesis of C27 and C29 *n*-alkanes, but also provides
241 C28 fatty acyl-CoA for BgElo12 to elongate to C30 fatty acyl-CoA, which in turn generates C29 *n*-alkane.
242 This might be the reason why *in vivo* RNAi of *BgElo12* slightly decreased C29 *n*-alkane and caused a
243 dramatic increase in C27 *n*-alkane, whereas RNAi of *BgElo24* dramatically decreased C29 *n*-alkane.
244 In order to analyze the activity of BgElo12 and BgElo24 in elongating methyl-branched FAs, two
245 representative substrates, 2-MeC16:0 and 14-MeC16:0 FAs, the potential substrates for 15-methyl HCs and
246 3-methyl HCs, respectively, were added to the medium. However, we found that these substrates could not
247 be catalyzed by BgElo12 or BgElo24 (Figure 4–figure supplement 1F–F'' and 1G–G''). We suspect that this
248 might be caused by a shortcoming of the yeast FA elongation system. FA elongation requires an elongase
249 and three other enzymes including a 3-keto-acyl-CoA-reductase, a 3-hydroxy-acyl-CoA dehydratase, and a
250 trans-enoyl-CoA-reductase (Wicker-Thomas et al., 2015). The last three yeast-endogenous enzymes may not
251 catalyze methyl branched substrates. In conclusion, these results indicate that both BgElo12 and BgElo24
252 catalyzed the biosynthesis of VLCFAs in the yeast heterologous system, and BgElo24 was able to provide
253 primary substrates for BgElo12. However, the activity of BgElo12 and BgElo24 in methyl-branched FA
254 elongation needs further investigation.
255

256 Female-enriched HCs are crucial for contact sex pheromone-based courtship 257 performance

258 The largest single chromatographic HC peak in females contains 3,7-; 3,9-; 3,11-DimeC29, which is
259 much less represented in males. Because 3,11-DimeC29 has been shown to be the precursor for the contact
260 sex pheromone 3,11-DimeC29-2-one (C29 methyl ketone) in *B. germanica* (Chase et al., 1992), we suspected
261 that the female-specific HC profile may be important for maintaining a high level of contact sex pheromone.
262 We first monitored the pattern of 3,11-DimeC29-2-one accumulation in the first gonotrophic cycle. The
263 contact sex pheromone showed a stable low level at the early adult stage (AD0–AD2), its accumulation
264 started at AD3, quickly increased from AD5 to AD7 (Figure 5A), but decreased at AD8 when most females

265 oviposited (data not shown). Analysis of the influence of *BgElo12*-RNAi on C29 methyl ketone was
266 performed at AD6. Female cockroaches were subjected for three consecutive dsRNA injections before being
267 subjected to lipid analysis: the first one at early fifth instar, the second at early sixth instar, and the third at
268 AD1. We found that repression of *BgElo12* reduced the C29 methyl ketone by more than 75% in both
269 cuticular and internal extractions (Figure 5B–D).

270 We next determined whether the *BgElo12*-RNAi repression of pheromone production in females
271 affected male courtship behavior. When the female contact sex pheromone is detected by a male, it displays
272 a characteristic male courtship behavior, including wing-raising (WR) (Eliyahu et al., 2008a). Importantly,
273 this behavior can be elicited by an isolated female antenna, and details of this assay, including latency and
274 rate of WR, have been described (Wada-Katsumata and Schal, 2019). When an antenna of AD5 female was
275 used as stimulus, nearly all males responded. RNAi of *BgElo12* resulted in only a slight decline in WR rate
276 (about 20%), but the latency of WR was significantly increased (Figure 5E and 5E'). AD5 females
277 accumulated a large amount of contact sex pheromone, whereas males can be fully activated by about 10 ng
278 of 3,11-DimeC29-2-one applied onto an antenna (Schal et al., 1990). This is likely the reason why RNAi of
279 *BgElo12* had only a small influence on WR rate. Therefore, we repeated this experiment using AD3 females,
280 which have less contact sex pheromone on the cuticle. We found that males responded to 80% of the control
281 antennae with the WR display, but less than 40% of the antennae from *BgElo12*-RNAi females elicited WR
282 in males. The average latency of WR toward antennae of *BgElo12*-RNAi females was 18.03 s, while the
283 control antennae elicited WR in 11.05 s (Figure 5F and 5F'). These results indicate that the female-enriched
284 HCs are advantageous for contact sex pheromone biosynthesis, especially at the early sexual maturation stage.
285

286 **Sex-differentiation genes modulate *BgElo12***

287 The female-enriched HC composition is tightly associated with a higher expression of *BgElo12* in
288 females, but the regulators that govern sexually dimorphic expression of *BgElo12* in females and males are
289 unknown. Wexler et al. (2019) reported that RNAi of the sex-determination gene *BgTra* in females converts
290 its CHC profile to a male-like profile. Taken together with our results, it would appear that the sex-
291 differentiation pathway might be involved in regulating *BgElo12* expression. We first confirmed the function
292 of *BgTra* and *BgDsx* in sex-specific development *via* RNAi. For each gene, we used two unique RNAi targets
293 within a conserved sequence region for multiple isoforms. RNAi of *BgTra* and *BgDsx* in females or males

294 showed similar phenotypes as described by Wexler et al. (2019). *BgTra* is only functional in females, while
295 *BgDsx* only works in males (Figure 6–figure supplement 1). We next studied the expression of *BgTra* and
296 *BgDsx* in females and males using qPCR primers that target all isoforms of each gene. The expression of
297 both *BgTra* and *BgDsx* increased after eclosion, but *BgTra* transcript levels tended to be stable from AD4 to
298 AD6 (Figure 6A–B). RNAi of *BgTra* in females significantly decreased the mRNA level of *BgElo12*, but
299 *BgElo12* expression was unaffected in males (Figure 6C). Notably, the downregulation of *BgElo12* by
300 ds*BgTra*-injection in females could be rescued by co-injection of ds*BgTra* and ds*BgDsx* (Figure 6C), but
301 ds*BgDsx* alone was not functional in regulating *BgElo12* expression in females (Figure 6D). Conversely, in
302 males, knockdown of *BgDsx* alone increased the expression of *BgElo12* (Figure 6D). According to Wexler
303 et al. (2019), RNAi of *BgTra* in females generated the male type *BgDsx* ($BgDsx^{M}$). We suspect that the
304 downregulation of *BgElo12* in females after RNAi of *BgTra* was caused by the generation of $BgDsx^{M}$. This
305 hypothesis was supported by co-injection of ds*BgTra* and ds*BgDsx*, and a dual-luciferase reporter assay that
306 $BgDsx^{M}$ could directly modulate the expression of *BgElo12* by interaction with its upstream sequence region
307 (Figure 6-figure supplement 2). Further, we found that RNAi of neither *BgTra* in females nor *BgDsx* in males
308 could affect the expression of *BgElo24* (Figure 6–figure supplement 3), suggesting that *BgElo24* is not
309 regulated by these two sex-differentiation genes.

310 We further analyzed the effects of *BgTra* and *BgDsx* on HC profiles. Knockdown of *BgTra* in females
311 masculinized the CHC profile and increased the male-enriched CHC components; however, this change
312 disappeared by co-injection of ds*BgTra* and ds*BgDsx* (Figure 6E–F, and Figure 6–figure supplement 4A).
313 Similarly, repression of *BgDsx* in males feminized the CHC profile, and increased the female-enriched
314 components (Figure 6E, 6G, and Figure 6–figure supplement 4B). In order to verify that the sex-
315 differentiation genes affected CHC profiles by regulating the generation of HCs but not their selective
316 transport and deposition to the cuticle, we analyzed the internal HCs. RNAi of both *BgTra* in females and
317 *BgDsx* in males caused an inter-sexual conversion of internal HC profiles, as seen in the CHCs (Figure 6–
318 figure supplement 5A–D). Although we found little qualitative differences in the HC profiles between
319 internal and cuticular HCs, we found significant quantitative changes. For example, after RNAi inhibition of
320 *BgTra* in females, the increase of 9-; 11-; 13-; 15-MeC29 (peak 17) on the epicuticle was greater than in
321 internal tissues, while the decrease of 3,7-; 3,9-; 3,11-DimeC29 (peak 24) on the surface was less than in
322 internal tissues (Figure 6–figure supplement 4A and Figure 6–figure supplement 5A), suggesting the

323 possibility of excessive transport of internal HCs toward the cuticle after repression of *BgTra* in females. As
324 for RNAi of *BgDsx*, an opposite change was generated in males– there appeared to be less transport of HCs
325 to the cuticle (Figure 6–figure supplement 4B, Figure 6–figure supplement 5B). Also, the total amount of
326 internal HCs was significantly decreased in *BgTra*-RNAi females, while it was increased in *BgDsx*-RNAi
327 males (Figure 6–figure supplement 5E and 5F). These results suggest that there is an unusual transport of
328 HCs after repression of *BgTar* or *BgDsx*. We suspect that the unusual transport of HCs may be caused by
329 changes in the capacity to store internal HCs, as large amounts of internal HCs are shunted to the ovaries
330 (Schal et al., 1994; Gu et al., 1995), and sex-differentiation genes are the key regulators of normal ovary
331 development in females and repression of ovary generation in males (Kopp, 2012; Wexler et al., 2019). We
332 conclude that although the transport of HCs from internal tissues to the cuticle was affected after repressing
333 *BgDsx* or *BgTra*, the effect was on overall HC transport, with no apparent selective transport on specific HCs.
334 Overall, our results indicate that the sexual dimorphism of HCs in *B. germanica* is primarily determined
335 by *BgElo12*, and sex-determination pathway genes are the critical regulators that control the asymmetric
336 expression of *BgElo12* between males and females.
337

338 # Discussion

339 Our study reveals a novel molecular mechanism responsible for the formation of SDHCs in *B.*
340 *germanica*. The CHC profiles in insects are regulated by complex biosynthetic and transport pathways,
341 involving multiple gene families. We demonstrated that a fatty acid elongation step is responsible for sexual
342 dimorphism of CHCs in *B. germanica*, the female-enriched *BgElo12* is the core gene that encodes for the
343 elongase involved in generating more female-enriched HCs, and the asymmetric expression of *BgElo12*
344 between the sexes is modulated by sex-differentiation genes: $BgDsx^M$ represses the expression of *BgElo12* in
345 males, while *BgTra* removes this repression in females. Because a female-enriched HC serves as a precursor
346 to a female contact sex pheromone, we also revealed the prominence of *BgElo12* in sexual behavior.
347

348 **Fatty acid chain elongation is a key step in the regulation of sexually dimorphic HCs in *B.***
349 ***germanica***

350 The diversity of HCs in insects is reflected in the HC carbon chain lengths, their degree of saturation,
351 and the number and positions of methyl groups (Holze et al., 2020). HCs in *B. germanica* are composed of
352 only alkanes and methyl-branched alkanes, and the fatty acid biosynthesis gene that governs the incorporation
353 of methyl groups in the aliphatic chain showed no role in generating the sexual dimorphism of HCs in *B.*
354 *germanica* (Pei et al., 2019). In this study, we found that sexually mature female cockroaches contain
355 relatively higher amounts of C29 HCs than males, whereas male cockroaches had more C27 HCs, suggesting
356 that chain length is an important factor in the dimorphism of HCs.

357 Studies of the genetic bases of HC biosynthesis in insects have demonstrated that chain lengths are
358 determined by the fatty acid elongation process: the rate-limiting enzyme elongase determines the chain
359 lengths of VLCFA products, and produces the final HCs with different chain lengths (Ginzel and Blomquist,
360 2016). In our study, an RNAi screen identified that *BgElo12* and *BgElo24* were involved in HC biosynthesis.
361 Expression of both genes in yeast demonstrated that both BgElo12 and BgElo24 displayed functions similar
362 to ELOVL4 in mammals, which showed a special function in the biosynthesis of VLCFAs with chain lengths
363 greater than C28 (Ohno et al., 2010). *BgElo24*, however, is a more fundamental elongase that seems able to
364 catalyze a wide range of substrates to generate FAs of various chain lengths, and can also provide primary
365 substrates for BgElo12 to produce C30 FAs. Notably, only *BgElo12* had higher expression in females, which

366 was consistent with the higher amounts of C29 HCs in females. Knockdown of *BgElo12* in females caused
367 a dramatic decrease of the female-enriched peak 24 (3,7-; 3,9-; 3,11-DimeC29) but it did not affect the male-
368 enriched peak 17 (9-; 11-; 13-; 15-MeC29), which generated a male-like HC profile; however, RNAi of
369 *BgElo24* unselectively downregulated all C28–30 HCs, indicating that only *BgElo12* was involved in the
370 formation of SDHCs in *B. germanica*. Lastly, we found both RNAi of *BgElo12* and *BgElo24* increased some
371 C27 HCs, indicating that there are some other *BgElos* involved in HC production. The identification of these
372 genes will be arduous, because the C27 compounds occur in small amounts, and multiple BgElos may
373 catalyze the synthesis of the same HC independently. It is worth noting in this regard that *Blattella asahinai*,
374 a sister species of *B. germanica* produces almost no C27 compounds (Pfannenstiel et al. 2008). These two
375 species can hybridize, potentially offering a resource for the genetic regulation of C27 HCs.

376 In *B. germanica*, as in other insects, HCs are transported through the haemolymph and selectively
377 incorporated into or deposited on various tissues, including the cuticle, ovaries and specialized pheromone
378 glands (Young et al., 2000; Schal et al., 2001; Schal et al. 1998). In our study, analysis of the influence of
379 *BgElo12*-RNAi on internal HCs demonstrated that the female- and male-specific CHC profiles were not
380 caused by selective transport, but rather by differences in *de novo* HC biosynthesis between the sexes,
381 regulated by *BgElo12*. Elongases have been shown to participate in HC production in several other insect
382 species including *D. melanogaster*, *Nilaparvata lugens*, and *Locusta migratoria* (Chertemps et al., 2007; Li
383 et al, 2019b; Zhao et al., 2020). The elongase gene *eloF* was also shown to be specifically expressed in
384 females, and might be associated with the sex-differentiation gene *Transformer*, but the reason why it cannot
385 be transcribed in male flies is not very clear (Chertemps et al., 2007). Nevertheless, the roles of elongase
386 genes in sexual dimorphism of HCs in other insects have not been described.

387

388 **$BgElo12$ and $BgDsx^M$ are key nodes connecting the hydrocarbon synthesis and sex-**
389 **differentiation pathways**

390 In this study, we first demonstrated that *BgElo12* is the key regulator in the HC biosynthesis pathway,
391 responsible for the differences in the HC profiles between females and males. We next explored the upstream
392 regulators that modulate the sexually dimorphic expression of *BgElo12*. The molecular genetic switches that
393 determine which sex-determination pathway is followed by males and females are highly variable in animals.
394 The *doublesex/mab-3 related* (*Dmrt*) family of transcription factors includes conserved developmental

395 regulators in the sex-differentiation pathway, governing the fate of sexually dimorphic traits in animals (Kopp,
396 2012). *Doublesx* (*Dsx*) in arthropods, which is related to *Dmrt*, works through sex-specific splice variants
397 that are controlled by *Tra* in many insects. Sex-specific *Dsx* isoforms promote sexual differentiation by
398 modulating diverse downstream genes; thus, the *Dsx* gene is regarded as a central nexus in sexual
399 differentiation (Gempe and Beye, 2011; Verhulst and van de Zande, 2015). Previous work reported that
400 knockdown of *BgTra* converted the female cockroach CHC profiles to male-like profiles (Wexler et al., 2019).
401 In our study, RNAi of *BgTra* in female cockroaches indeed downregulated the expression of *BgElo12*, but
402 the effect of *BgTra*-RNAi on *BgElo12* expression could be recovered by co-injection of ds*BgTra* and
403 ds*BgDsx*, and RNAi of *BgDsx* in males upregulated *BgElo12* transcripts. These results suggest that $BgDsx^M$
404 can repress the transcription of *BgElo12* in males, and the downregulation of *BgElo12* by repressing *BgTra*
405 was caused by the conversion of $BgDsx^F$ to $BgDsx^M$, as *BgTra* is able to regulate the splicing of $BgDsx^M$ to
406 $BgDsx^F$ (Wexler et al., 2019). The regulation of *BgElo12* by *BgDsx* connects the sex-differentiation pathway
407 with the HC biosynthesis pathway, and therefore enables the sexual dimorphism of HCs in *B. germanica*.

408 Although the dual-luciferase reporter gene assay suggested that $BgDsx^M$ can directly regulate the
409 transcript of *BgElo12*, there may be other indirect regulatory pathways. Several candidate factors have been
410 shown to regulate the HC profiles in various insects (e.g., *D. melanogaster*), including ecdysone, juvenile
411 hormone (JH), biogenic amines, and the insulin signaling pathway (Wicker et al., 1995a; 1995b; Marican et
412 al., 2004; Kuo et al., 2012; Bontonou et al., 2015; Fedina et al., 2017; Baron et al., 2018). These connections
413 are highlighted by ecdysone, which is mainly produced by the prothoracic gland, but in some insects also by
414 the ovaries (Bownes and Smith, 1984; Romaá et al., 1995), and the development of the ovaries is under the
415 regulation of the sex-differentiation pathway. Moreover, endocrine signals like JH and insulin are also
416 regulated by the sex-differentiation pathway (Zinna et al., 2018). Therefore, these signals may be potential
417 mediators that complete the regulatory network between *BgDsx* and *BgElo12*. However, more detailed
418 investigations are needed to thoroughly elucidate the differential regulation of HC production in both females
419 and males.

420 *Dsx* also regulates the HC biosynthesis pathway in *D. melanogaster*; Dsx^F specifically activates the
421 transcription of *desatF* and generates pheromonal dialkenes (Shirangi et al., 2009). In *B. germanica*, *BgDsx*
422 operates differently in that $BgDsx^M$ suppresses female traits in male cockroaches, and *BgTra* is important in
423 removing this inhibitory effect in females (Wexler et al., 2019). Thus, $BgDsx^M$ represses the expression of

424 *BgElo12*, and therefore it represses the generation of female-enriched HCs in males, and *BgTra* is crucial in
425 maintaining female-enriched HCs, especially for the contact sex pheromone precursors. However, *BgTra*
426 affects contact sex pheromone biosynthesis in female cockroaches through additional pathways. We found
427 that RNAi of *BgTra* in females dramatically decreased the expression of the JH-responsive *Krüppel homolog*
428 *1*, *Krh1*, a zinc-finger transcription factor (Figure 6–figure supplement 6). JH can activate the expression of
429 a putative sex-specific and rate-limiting cytochrome p450 that catalyzes the hydroxylation of 3,11-DimeC29
430 to 3,11-DimeC29-alcohol, which is then oxidized to the methyl ketone pheromone (Chase et al., 1992;
431 Lozano and Belles, 2011), and we found that JH performed this function *via Krh1* (our unpublished data).
432 Therefore, the influence of *BgTra* on contact sex pheromone biosynthesis is explained not only by its effects
433 on precursor synthesis, but also by the transition of precursors to methyl ketones.
434

435 **Biological significance of the sexual dimorphism of HCs**

436 Sexually dimorphic traits are generated in females and males in response to intra- and inter-sexual
437 selection, but pleiotropic traits are also subject to natural selection, especially when they are also shaped by
438 and adapted to environmental stresses (Andersson, 1994; Kunte, 2008). Most insect sex pheromones are C12-
439 18 aldehydes, alcohols and acetate esters, derived from fatty acids in specialized pheromone glands. These
440 pheromones appear to have no other function beyond attracting the opposite sex. In contrast, CHC
441 pheromones appear to serve both in sexual communication and in waterproofing of the cuticle. The female-
442 specific contact sex pheromone of *B. germanica* is clearly subject to both natural and sexual selection because
443 it is derived from a prominent CHC, which also serves as a waterproofing component of the CHC profile and
444 is maternally invested in offspring (Fan et al., 2008). Thus, maintenance of HC contact sex pheromone
445 precursors in female cockroaches is adaptive in both reproductive success and survival in an arid environment.
446 The quality of insect pheromones is considered an honest indicator of fitness potential (Kuo et al., 2012).
447 This assertion may be particularly pertinent in *B. germanica*, where the pheromone and its HC precursor
448 serve in sexual communication, resilience to environmental stressors, and in maternal investment in eggs.

449 In systems that use CHCs in sexual communication, it is common for the CHC profiles to contain
450 female- and male-specific components, as is evident in *Drosophila*. In *B. germanica*, as well, male
451 cockroaches have a unique CHC profile, especially enriched in C27 components with 9-; 11-; 13-; 15-MeC29
452 being particularly prominent. The male-specific HC profile is generated during sexual maturation, suggesting

453 that it may function in sexual communication. It is possible that the male-enriched 9-; 11-; 13-; 15-MeC29
454 may function as a sex pheromone in three related contexts: a) it may distinguish males and females within
455 cockroach aggregations; b) it may signal “maleness” and male quality to females; and c) it may function in
456 male-male recognition, contests and competition for access to females. Moreover, it is possible that male-
457 specific P450s may catalyze the oxidation of these male-enriched HCs to homologous methyl ketones, as in
458 females, and in turn serve these functions. However, more bioassays are required to analyze the biological
459 significance of male-specific CHC profiles.

460 # Materials and Methods

461 ## Insect rearing

462 The German cockroach, *Blattella germanica* originated from a laboratory strain collected in the 1970s.
463 The cockroaches were maintained in aquaria at 30 ± 1ºC with a relative humidity (RH) of ~ 50% under 12:
464 12 h light–dark photoperiod regime, and fed rat chow and tap water. Newly hatched cockroaches were
465 separated and reared in new containers. Early stage (day 1 or 2) fourth- and fifth-instar nymphs were
466 separated and used in dsRNA injection; newly emerged adults were collected and reared in plastic jars for
467 experiments.

468

469 ## Preparation of HCs and methyl ketones

470 *Blattella germanica* cuticular lipids were extracted following Gu et al. (1995) with slight modifications.
471 Individual adult female cockroaches were sacrificed by freezing at −20ºC, thawed at room temperature, the
472 cuticle surface-extracted in 1 mL of hexane twice, and finally rinsed in 1 mL of hexane. *n*-Hexacosane (15
473 μg) or 14-heptacosanone (0.5 μg) were added as internal standards. The extracts were combined and reduced
474 to ~300 μL with a nitrogen flow and loaded onto a Pasteur pipette silica gel mini-column, as previously
475 described (Pei et al., 2019). The cuticular hydrocarbons were eluted with 8 mL of hexane, and the contact
476 sex pheromone fraction was subsequently eluted with 8 mL of 3% ethyl ether in hexane. Internal lipids were
477 extracted from the cockroach following a procedure described by Fan et al. (2002) with slight modifications.
478 Each surface-extracted cockroach was homogenized in a solution of hexane–methanol–ddH2O (2:1:1 mL),
479 30 μg of *n*-hexacosane and 1 μg of 14-heptacosanone were added for quantification of internal HCs and
480 methyl ketones, respectively. The homogenate was vigorously vortexed and centrifuged at 2500 g for 10 min.
481 The supernatant hexane phase was collected and the extraction was repeated using n-hexane. Separation of
482 HCs and methyl ketones was performed using column chromatography, as described above.

483

484 ## Gas chromatography–mass spectrometry (GC–MS) analysis

485 Lipid analysis was performed with a TRACE 1310 GC–ISQ single quadrupole MS (Thermo Fisher
486 Scientific, Waltham, MA, USA). In brief, lipids were separated on a DB-5MS capillary column (30 m length,
487 0.25 mm ID, 0.25 μm film thickness; Agilent Technologies, Santa Clara, CA, USA). The oven started at

488 60°C and kept for 2 min, heated to 160°C for HCs and methyl ketones, or 220°C for fatty acid methyl esters
489 (FAMEs) at a rate of 30°C/min, then increased at 3°C/min up to 250°C, followed by 10°C/min up to 320°C
490 and held for 5 min. Electron ionization mode (70 eV) was used, and the MS scan range was 45–650 m/z at a
491 rate of 5 scans/s. Identification of compounds and peak area determination was performed with a Xcalibur
492 2.2 workstation.
493

494 **RNA isolation and real time-quantitative PCR (RT-qPCR)**

495 Total RNA was isolated with RNAiso Plus Reagents (Takara, Dalian, Liaoning, China) according to the
496 manufacturer's instructions. cDNA was reverse-transcribed from 800 ng of total RNA using the
497 PrimeScript™ RT reagent Kit with gDNA Eraser (Takara). Gene-specific primers with appropriate
498 amplification efficiency (0.95–1.05) were screened by a cDNA dilution series (Supplementary file 2).
499 Quantification of gene expression level was performed with TB Green™ Premix Ex Taq™ Tli RNase H Plus
500 (Takara) on a LightCycler 480 system (Roche). Target genes expression was normalized by the commonly
501 used housekeeping gene *actin5c* (GenBank: AJ862721.1) and calculated using the $2^{-\Delta\Delta Ct}$ method (Livak and
502 Schmittgen, 2001). Each treatment contained four biological replicates and technical triplicates.
503

504 **Identification of *BgElo* gene family members**

505 Both BLASTN and BLASTP were used to search *BgElo* genes in *B. germanica* genome data (Harrison
506 et al., 2018) and our own full-length transcriptome data (NCBI accessions: SRR9143014 and SRR9143013)
507 using the homologous genes of *Elongase* from *D. melanogaster* as query sequences. Candidate *BgElo* genes
508 were amplified with the PrimeSTAR GXL DNA Polymerase reagent (Takara) (primers are listed in
509 supplementary file 2), the amplified fragments were inserted into the pMD™ 19-T Vector (Takara) and re-
510 sequenced. Candidate *BgElo* genes were then translated and submitted to SMART online tools
511 (http://smart.embl-heidelberg.de) to analyze the conserved structures; only genes with the typical ELO
512 domain were confirmed as *BgElo* genes. The putative *BgElo* mRNA sequences were mapped to the genomic
513 data (GenBank: PYGN00000000.1) using a local BLASTN tool (Altschul et al. 1990), and the intron-exon
514 structure was analyzed based on the GT-AG rule. The conservative motifs in *BgElos* were analyzed by
515 sequence alignment with DNAMAN 9.0 software.
516

517 **Expression profile analysis**

518 In order to screen the potential *BgElo* genes involved in HC biosynthesis, the expression levels of
519 different *BgElo* genes were quantified in the fat body and abdominal integument, where HCs or their
520 precursors were generated. In addition, other tissues including the head, thorax, gut, legs, ovaries, Malpighian
521 tubules, ejaculatory duct (from two-day-old males), and colleterial glands were dissected from two-day-old
522 females, and were used to analyze the expression profiles of *BgElo12* and *BgElo24* among different tissues.
523 In order to study the time course of *BgElo12*, *BgElo24*, *BgDTra*, and *BgDsx* transcript levels during sexual
524 maturation, a representative nymphal stage (4-day-old sixth-instar nymph, N6D4) and AD0–AD6 females
525 and males were collected. Total RNA was extracted from various tissues or intact cockroaches, and the
526 expression profiles of different genes were studied *via* RT-qPCR.

527

528 **Transcript knockdown *via* RNAi**

529 Gene-specific target sequences as well as a heterologous fragment from *Mus musculus* (Muslta) used
530 for double-stranded RNA (dsRNA) synthesis were amplified and cloned into pMD^{TM} 19-T Vector (Takara).
531 Templates used for single-stranded RNA were amplified with primers that incorporated with the T7 promoter
532 sequence (Supplementary file 2). Different kinds of dsRNA were subsequently generated with the T7
533 RiboMAX™ Express RNAi System (Promega). Delivery of dsRNA was performed with a Nanoject II micro-
534 injector (Drummond Scientific) for fourth-instar cockroaches and microliter syringes for fifth-, sixth-instar,
535 and adult cockroaches. For RNAi screen of *BgElo* genes in HC biogenesis, a double injection strategy was
536 employed: the first injection was performed at the early fifth-instar (1- or 2-day-old fifth-instar, N5D1-N5D2)
537 with a dosage of 3 μg in 2 μL; the second injection was performed one week later with a dosage of 4 μg in 2
538 μL. For confirming the function of *BgElo12* in contact sex pheromone biosynthesis, a third injection with 4
539 μg of dsRNA in 2 μL was carried out on 1-day-old adults (AD1), and methyl ketones were extracted at AD6.
540 Knockdown of sex-determination genes was accomplished with three dsRNA injections, the first at early
541 fourth instar (N4D1-N4D2), the second at early fifth instar (N5D1-N5D2), and the last at early sixth instar
542 (N6D1-N6D2). The fourth-instar cockroaches were injected with ~0.5 μg of dsRNA in ~0.2 μL; the fifth-
543 and sixth-instar cockroaches were injected with 1 μg of dsRNA in 2 μL. In order to verify the function of
544 *BgElo12* and *BgElo24* in HC biosynthesis and sex-determination genes in modulating *BgElo12* mRNA levels
545 or HC profiles, two non-overlapping gene-specific targets were designed and used in this study, as there are

546 some isoforms of *BgDsx* and *BgTra*, the RNAi targets were designed within the common sequence region
547 according to Wexler et al. (2019).
548

549 **Heterologous expression and fatty acid analysis**

550 Heterologous expression was performed according to Hastings et al. (2001) with slight modifications.
551 Complete coding sequences (CDS) of *BgElo12*, *BgElo24*, or control (*GFP*) were amplified with
552 PrimeSTAR® HS DNA Polymerase (Takara) using gene-specific primers (Supplementary file 2) that contain
553 the restriction enzyme sites (*KpnI* and *BamHI* for *BgElo12* and *BgElo24*; *BmHI* and *EcoRI* for *GFP*) and the
554 yeast consensus sequence (TACACA) following the restriction enzyme sites (only for forward primers). The
555 amplified *BgElo12*, *BgElo24*, or *GFP* CDS fragments were ligated into the linearized pYES2 shuttle plasmid
556 (Thermo Fisher Scientific) and verified by sequencing. The recombinant plasmids were transformed into
557 INVSc1 *Saccharomyces cerevisiae* (Thermo Fisher Scientific) using the PEG-LiAc method, and streaked
558 onto *S. cerevisiae* minimal medium minus uracil (SC-Uracil) plates to select transformants; single colonies
559 were inoculated in SC-Uracil medium with 2% glucose. After culturing at 30℃ for 24 h, the yeast was
560 collected and diluted to an OD600 of 0.4 with SC–Uracil medium containing 1% raffinose and 2% galactose,
561 and further cultured at 30℃ until they reached an OD600 of 0.8. At this point, transcription of exogenous
562 genes was examined by RT-PCR. Substrates of C20 (0.5 mM), C22 (1 mM), C24 (1 mM), C26 (1 mM), C28
563 (1 mM), 2-methylhexadecanoic acid (0.5 mM), and 14-methylhexadecanoic acid (0.5 mM) were separately
564 added into the cultures with an extra 1% of tergitol type Nonidet P-40. All the substrates were purchased
565 form Sigma-Aldrich (Louis, MO, USA) or TCI (Shanghai, China).

566 After 48 h, yeast cells were harvested by centrifugation at 500 g for 5 min and washed thrice with Hank's
567 balanced salt solution for fatty acid derivatization and analysis. Pellets were dried under a steam of nitrogen
568 and 2 mL of 1% (v/v) H_2SO_4 in methanol was added, the mixture was vortexed and incubated at 80°C in a
569 N_2 atmosphere for 2 h (Lepage and Roy, 1984). After that, 1 ml of saturated sodium chloride solution was
570 added into the mixture and FAMEs were extracted with 1 mL of hexane three times. The FAME extracts
571 were concentrated and subjected to GC–MS analysis as described above. Different FAMEs were identified
572 by comparison to FAME standards (purchased from Sigma-Aldrich) and their mass spectra.
573

574 **Desiccation bioassay**

575 The capacity of *BgElo12* and *BgElo24* to contribute to water retention was assessed by a desiccation
576 bioassay. Drying bottles were prepared by putting ~120 g of packed fresh silica gel into a ~900 mL sealed
577 plastic bottle. The RH inside the bottle dropped to 5% within 2 h which was monitored by HOBO Pro v2
578 (Onset, Bourne, USA). AD2 females were injected with ds*BgElo12*, ds*BgELo24*, and ds*Muslta* and
579 separately caged in the desiccation bottles at 30℃, supplied with ~1 g of dry food, but no water. Survival
580 was recorded every 8 h until all the cockroaches died. About 100 cockroaches were used for each treatment.
581

582 **Courtship behavioral study**

583 Courtship behavior was tested according to Eliyahu et al. (2008b) with slight modifications. Antennae
584 from differently treated AD3 or AD5 females were excised, and each antenna was attached to the tip of a
585 glass Pasteur pipette with paraffin, the antenna was used immediately to test the responses of AD13–15 males
586 that were separated from females since eclosion. The test antenna was used to touch the antennae of the male,
587 and a positive response was recorded if the male cockroach turned its body and raised the wings to
588 approximately 90 degrees within 30 sec. A negative response was recoded if the test antenna failed to elicit
589 a response in a male cockroach and this male then responded to a positive control antenna from a normal
590 AD6 female. The wing raising (WR) latency was recorded according to Wada-Katsumata and Schal (2019);
591 the latency of the WR display was timed from contact of the antennae to the initiation of the male WR display.
592 All female antennae and male cockroaches were used only once, all tests were performed in the scotophase
593 and we avoided the first and last 2 h of the scotophase. Bioassays were conducted under a dim red light to
594 simulate a dark environment.
595

596 **Dual-luciferase reporter gene assay**

597 The 5' end of *BgElo12* was obtained by 5' Rapid Amplification of cDNA Ends (RACE). 5' RACE
598 cDNA library was prepared using Clontech SMARTer RACE 5'/3' Kit (Takara) according to the user manual
599 with the gene-specific primer (Supplementary file 2) and kit-provided Universal long primer. The amplified
600 fragments were cloned into pRACE vector and sequenced. About a 2.7 kb sequence upstream of *BgElo12*
601 was amplified and cloned into pGL3-basic vector, and the CDS sequences of $BgDsx^{M}$ and GFP (control)
602 were separately cloned into the expression vector pCDNA3.1. The HEK293T cells were cultured in a 24-
603 well plate with 500 μL of DMEM medium (Thermo Fisher Scientific) for 24 h before transfection, and the

604 restructured pGL3-basic vector (200 ng/well) was co-transfected with the expression vectors (200 ng/well)
605 to HEK293T cells using Lipofectamine™ 3000 (Invitrogen, Carlsbad, CA, USA). The pRL-TK that encoded
606 a *Renilla* luciferase was also co-transfected as an internal control. The transfected cells were cultured at 37°C
607 for 36 h and subjected to luciferase activity analysis using the Dual-Glo Luciferase Assay System (Promega,
608 Madison, WI, USA).
609

610 **Statistics**

611 Data were statistically analyzed using SPSS 23 and presented as mean ± SEM or mean ± SD.
612 Two-tailed Student's *t*-test was used for two-group comparison; significant differences between multi-groups
613 were analyzed by one-way ANOVA followed by the LSD test (Equal variances assumed) or Welch's
614 ANOVA followed by Games-Howell multiple comparisons test (Equal variances not assumed) at $P < 0.05$
615 level. Principal component analysis (PCA) was used to distinguish the CHC profiles of AD1 and AD6
616 cockroaches.
617

Acknowledgments

We thank Shan-Wang Hong from Northwest A&F University for his help in sequence analysis. This work was supported in part by the National Natural Science Foundation of China to YLF (Grant No. 31772533), the United States National Science Foundation (IOS-1557864), the Blanton J. Whitmire Endowment at North Carolina State University to CS, and the Special Fund of Northwest A&F University to TXL (NWAFU-2009-01-001-TXL).

Competing interests: The authors declare that no competing interests exist.

Additional information

Funding

Funder	Grant reference number	Author
National Natural Science Foundation of China	Grant No. 31772533	Yong-Liang Fan
United States National Natural Science	IOS-1557864	Coby Schal
Northwest A&F University Special Fund	2009-01-001-TXL	Tong-Xian Liu

The funders had no role in study design, data collection and interpretation, or the decision to submit the work for publication.

Author contributions

XJP, Conceptualization, Methodology, Investigation, Collection and analysis of data, Writing—original draft, Writing—review and editing; YLF, Funding acquisition, Conceptualization, Project administration, Writing—review and editing; YB, TTB, ZFZ, NC, Methodology, Investigation, Writing—review and editing; CS, Funding acquisition, Conceptualization, Writing—review and editing; SL, Resources, Methodology, Writing—review and editing; TXL, Funding acquisition, Resources, Supervision, Project administration,

Writing—review and editing.

Author ORCIDs and Emails:

Tong-Xian Liu: txliu@nwafu.edu.cn, 0000-0002-7686-0686

Yong-Liang Fan: yfan@nwafu.edu.cn, 0000-0002-7993-2497

Xiao-Jin Pei: xiaojinpei@nwafu.edu.cn, 0000-0003-4311-6954

Coby Schal: coby@ncsu.edu, 0000-0001-7195-6358

Data availability

PacBio data sets have been deposited in NCBI's SRA under the accession numbers SRR9143014 and SRR9143013. All *BgElo* sequences have been submitted to NCBI's GenBank under the accession numbers MT925720 and MW380216–MW380238

Additional files

Supplementary file 1. Sequence alignments and protein structure analysis of BgElos.

Supplementary file 2. Primer sequences used in this study.

655 ## References

656 Altschul SF, Gish W, Miller W, Myers EW, Lipman DJ. 1990. Basic local alignment search tool. *J Mol*
657 *Biol* 215:403–410. DOI: https://doi.org/10.1016/S0022-2836(05)80360-2.

658 Andersson M. 1994. Sexual selection. Princeton, NJ: Princeton University Press.

659 Baron A, Denis B, Wicker-Thomas C. 2018. Control of pheromone production by ovaries in *Drosophila*. *J*
660 *Insect Physiol* 109:138–143. DOI: https://doi.org/10.1016/j.jinsphys.2018.07.003.

661 Bear A, Monteiro A. 2013. Both cell-autonomous mechanisms and hormones contribute to sexual
662 development in vertebrates and insects. *BioEssays* 35:725–732. DOI:
663 https://doi.org/10.1002/bies.201300009.

664 Berson JD, Simmons LW. 2018. A costly chemical trait: phenotypic condition dependence of cuticular
665 hydrocarbons in a dung beetle. *J Evol Biol* 31:1772–1781. DOI: https://doi.org/10.1111/jeb.13371.

666 Berson JD, Garcia-Gonzalez F, Simmons LW. 2019. Experimental evidence for the role of sexual selection
667 in the evolution of cuticular hydrocarbons in the dung beetle, *Onthophagus taurus*. *J Evol Biol*
668 32:1186–1193. DOI: https://doi.org/10.1111/jeb.13519.

669 Blomquist GJ, Tillman JA, Reed JR, Gu P, Vanderwel D, Choi S, Reitz RC. 1995. Regulation of enzymatic
670 activity involved in sex pheromone production in the housefly, *Musca domestica*. *Insect Biochem Mol*
671 *Biol* 25:751–757. DOI: https://doi.org/10.1016/0965-1748(95)00015-n.

672 Blomquist GJ, Bagnères AG. 2010. Insect hydrocarbons: biology, biochemistry, and chemical ecology.
673 Cambridge University Press, New York, USA.

674 Blomquist GJ, Ginzel MD. 2021. Chemical ecology, biochemistry, and molecular biology of insect
675 hydrocarbons. *Annu Rev Entomol* 66:45–60. DOI: https://doi.org/10.1146/annurev-ento-031620-
676 071754.

677 Bontonou G, Shaik HA, Denis B, Wicker-Thomas, C. 2015. Acp70A regulates *Drosophila* pheromones
678 through juvenile hormone induction. *Insect Biochem Mol Biol* 56:36–49. DOI:
679 https://doi.org/10.1016/j.ibmb.2014.11.008.

680 Bownes M, Smith T. 1984. Ecdysteroids in adult males and females of *Drosophila melanogaster*. *J Insect*
681 *Physiol* 30:823–830. DOI: https://doi.org/10.1016/0022-1910(84)90019-2.

682 Chase J, Jurenka RA, Schal C, Halarnkar PP, Blomquist GJ. 1990. Biosynthesis of methyl branched
683 hydrocarbons of the German cockroach *Blattella germanica* (L.) (Orthoptera, Blattellidae). *Insect*

684 *Biochem* 20:149-156. DOI: https://doi.org/10.1016/0020-1790(90)90007-H.
685 Chase J, Touhara K, Prestwich GD, Schal C, Blomquist GJ. 1992. Biosynthesis and endocrine control of
686 the production of the German cockroach sex pheromone 3,11-dimethylnonacosan-2-one. *Proc Natl*
687 *Acad Sci USA* 89:6050–6054. DOI: https://doi.org/10.1073/pnas.89.13.6050.
688 Chen N, Pei XJ, Li S, Fan YL, Liu TX. 2020. Involvement of integument-rich *CYP4G19* in hydrocarbon
689 biosynthesis and cuticular penetration resistance in *Blattella germanica* (L.). *Pest Manag Sci* 76:215–
690 226. DOI: https://doi.org/10.1002/ps.5499.
691 Chertemps T, Duportets L, Labeur C, Ueyama M, Wicker-Thomas C. 2006. A female specific desaturase
692 gene responsible for diene hydrocarbon biosynthesis and courtship behaviour in *Drosophila*
693 *melanogaster*. *Insect Mol Biol* 15:465–473. DOI: https://doi.org/10.1111/j.1365-2583.2006.00658.x.
694 Chertemps T, Duportets L, Labeur C, Ueda R, Takahashi K, Saigo K, Wicker-Thomas C. 2007. A female-
695 biased expressed elongase involved in long-chain hydrocarbon biosynthesis and courtship behavior in
696 *Drosophila melanogaster*. *Proc Natl Acad Sci USA* 104: 4273–4278.
697 https://doi.org/10.1073/pnas.0608142104.
698 Chung H, Loehlin DW, Dufour HD, Vaccarro K, Millar JG, Carroll SB. 2014. A single gene affects both
699 ecological divergence and mate choice in *Drosophila*. *Science* 343:1148–1151. DOI:
700 https://doi.org/10.1126/science.1249998.
701 Chung H, Carroll SB. 2015. Wax, sex and the origin of species: Dual roles of insect cuticular hydrocarbons
702 in adaptation and mating. *BioEssays* 37:822–830. DOI: https://doi.org/10.1002/bies.201500014.
703 Clough E, Jimenez E, Kim YA, Whitworth C, Neville MC, Hempel LU, Pavlou HJ, Chen ZX, Sturgill D,
704 Dale RK, Smith HE, Przytycka TM, Goodwin SF, Van Doren M, Oliver B. 2014. Sex- and tissue-
705 specific functions of *Drosophila* doublesex transcription factor target genes. *Dev Cell* 31:761–773.
706 DOI: https://doi.org/10.1016/j.devcel.2014.11.021.
707 Connallon T, Knowles LL. 2005. Intergenomic conflict revealed by patterns of sex-biased gene expression.
708 *Trends Genet* 21:495–499. DOI: https://doi.org/10.1016/j.tig.2005.07.006.
709 Darwin C. 1871. The descent of man, and selection in relation to sex. London, UK: J. Murray.
710 Eliyahu D, Nojima S, Mori K, Schal C. 2008a. New contact sex pheromone components of the German
711 cockroach, *Blattella germanica*, predicted from the proposed biosynthetic pathway. *J Chem Ecol*
712 34:229–237. DOI: https://doi.org/10.1007/s10886-007-9409-8.

713 Eliyahu D, Nojima S, Capracotta SS, Comins DL, Schal, C. 2008b. Identification of cuticular lipids
714 eliciting interspecific courtship in the German cockroach, *Blattella germanica*. *Naturwissenschaften*
715 95:403–412. DOI: https://doi.org/10.1007/s00114-007-0339-7.
716 Eliyahu D, Nojima S, Mori K, Schal C. 2009. Jail baits: how and why nymphs mimic adult females of the
717 German cockroach, *Blattella germanica*. *Anim Behav* 78:1097–1105. DOI:
718 https://doi.org/10.1016/j.anbehav.2009.06.035.
719 Fan YL, Chase J, Sevala VL, Schal C. 2002. Lipophorin-facilitated hydrocarbon uptake by oocytes in the
720 German cockroach *Blattella germanica* (L.). *J Exp Biol* 205:781–790. DOI:
721 https://jeb.biologists.org/content/205/6/781.
722 Fan YL, Eliyahu D., Schal C. 2008. Cuticular hydrocarbons as maternal provisions in embryos and nymphs
723 of the cockroach *Blattella germanica*. *J Exp Biol* 211: 548-554. DOI:
724 https://jeb.biologists.org/content/211/4/548.
725 Fedina TY, Arbuthnott D, Rundle HD, Promislow D, Pletcher SD. 2017. Tissue-specific insulin signaling
726 mediates female sexual attractiveness. *PLoS Genet* 13:e1006935. DOI:
727 https://doi.org/10.1371/journal.pgen.1006935.
728 Ferveur JF, Sureau G. 1996. Simultaneous influence on male courtship of stimulatory and inhibitory
729 pheromones produced by live sex-mosaic *Drosophila melanogaster*. *Proc R Soc B* 263:967–973. DOI:
730 https://doi.org/10.1098/rspb.1996.0143.
731 Ferveur JF, Savarit F, O'Kane CJ, Sureau G, Greenspan RJ, Jallon JM. 1997. Genetic feminization of
732 pheromones and its behavioral consequences in *Drosophila* males. *Science* 276:1555–1558. DOI:
733 https://doi.org/10.1126/science.276.5318.1555.
734 Gempe T, Beye M. 2011. Function and evolution of sex determination mechanisms, genes and pathways in
735 insects. *BioEssays* 33:52–60. DOI: https://doi.org/10.1002/bies.201000043.
736 Gibbs AG, 1998. Water-proofing properties of cuticular lipids. *Am Zool* 38:471–482. DOI:
737 https://doi.org/10.1093/icb/38.3.471.
738 Ginzel MD, Blomquist GJ. 2016. Insect hydrocarbons: biochemistry and chemical ecology. In: Cohen, E.,
739 Moussian, B. (Eds.), Extracellular Composite Matrices in Arthropods. Springer, pp. 221–252.
740 Gu X, Quilici D, Juarez P, Blomquist GJ, Schal C. 1995. Biosynthesis of hydrocarbons and contact sex
741 pheromone and their transport by lipophorin in females of the German cockroach (*Blattella*

742 *germanica*). *J Insect Physiol* 41:257–267. DOI: https://doi.org/10.1016/0022-1910(94)00100-U.
743 Hall AB, Basu S, Jiang X, Qi Y, Timoshevskiy VA, Biedler JK, Sharakhova MV, Elahi R, Anderson MA,
744 Chen XG, Sharakhov IV, Adelman ZN, Tu Z. 2015. A male-determining factor in the mosquito *Aedes*
745 *aegypti*. *Science* 348:1268–1270. DOI: https://doi.org/10.1126/science.aaa2850.
746 Harrison MC, Jongepier E, Robertson HM, Arning N, Bitard-Feildel T, Chao H, Childers CP, Dinh, H,
747 Doddapaneni H, Dugan S, Gowin J, Greiner C, Han Y, Hu H, Hughes DST, Huylmans AK, Kemena C,
748 Kremer LPM, Lee SL, Lopez-Ezquerra A, Mallet L, Monroy-Kuhn JM, Moser A, Murali SC, Muzny
749 DM, Otani S, Piulachs MD, Poelchau M, Qu J, Schaub F, Wada-Katsumata A, Worley KC, Xie Q, Ylla
750 G, Poulsen M, Gibbs RA, Schal C, Richards S, Belles X, Korb J, Bornberg-Bauer E. 2018.
751 Hemimetabolous genomes reveal molecular basis of termite eusociality. *Nat Ecol Evol* 2:557–566.
752 DOI: https://doi.org/10.1038/s41559-017-0459-1.
753 Hasselmann M, Gempe T, Schiøtt M, Nunes-Silva CG, Otte M, Beye M. 2008. Evidence for the
754 evolutionary nascence of a novel sex determination pathway in honeybees. *Nature* 454:519–522. DOI:
755 https://doi.org/10.1038/nature07052.
756 Hastings N, Agaba M, Tocher DR, Leaver MJ, Dick JR, Sargent JR, Teale AJ. 2001. A vertebrate fatty acid
757 desaturase with Delta 5 and Delta 6 activities. *Proc Natl Acad Sci USA* 98:14304–14309. DOI:
758 https://doi.org/10.1073/pnas.251516598.
759 Herpin A, Schartl M. 2015. Plasticity of gene-regulatory networks controlling sex determination: of
760 masters, slaves, usual suspects, newcomers, and usurpators. *EMBO Rep* 16:1260–1274. DOI:
761 https://doi.org/10.15252/embr.201540667.
762 Holze H, Schrader L, Buellesbach J. 2020. Advances in deciphering the genetic basis of insect cuticular
763 hydrocarbon biosynthesis and variation. *Heredity*: In press. DOI: https://doi.org/10.1038/s41437-020-
764 00380-y.
765 Howard RW, Blomquist GJ. 2005. Ecological, behavioral, and biochemical aspects of insect hydrocarbons.
766 *Annu Rev Entomol* 50:371–393. DOI: https://doi.org/10.1146/annurev.ento.50.071803.130359.
767 Ingleby FC, Innocenti P, Rundle HD, Morrow EH. 2014. Between-sex genetic covariance constrains the
768 evolution of sexual dimorphism in *Drosophila melanogaster*. *J Evol Biol* 27:1721–1732. DOI:
769 https://doi.org/10.1111/jeb.12429.
770 Innocenti P, Morrow EH. 2010. The sexually antagonistic genes of *Drosophila melanogaster*. *PLoS Biol*

771 8:e1000335. DOI: https://doi.org/10.1371/journal.pbio.1000335.
772 Juárez MP, Chase J, Blomquist GJ. 1992. A microsomal fatty acid synthetase from the integument of
773 *Blattella germanica* synthesizes methyl-branched fatty acids, precursors to hydrocarbon and contact
774 sex pheromone. *Arch Insect Biochem Physiol* 293:333–341. DOI: https://doi.org/10.1016/0003-
775 9861(92)90403-j.
776 Juárez MP, Ayala S, Brenner RR. 1996. Methyl-branched fatty acid biosynthesis in *Triatoma infestans*.
777 *Insect Biochem Mol Biol* 26:599–605. DOI: https://doi.org/10.1016/S0965-1748(96)00021-5.
778 Juárez MP. 2004. Fatty acyl-CoA elongation in *Blatella germanica* integumental microsomes. *Arch Insect*
779 *Biochem Physiol* 56: 170–178. DOI: https://doi.org/10.1002/arch.20007.
780 Jurenka RA, Schal C, Burns E, Chase J, Blomquist GJ. 1989. Structural correlation between cuticular
781 hydrocarbons and female contact sex pheromone of German cockroach *Blattella germanica* (L.). *J*
782 *Chem Ecol* 15:939–949. DOI: https://doi.org/10.1007/BF01015189.
783 Kiuchi T, Koga H, Kawamoto M, Shoji K, Sakai H, Arai Y, Ishihara G, Kawaoka S, Sugano S, Shimada T,
784 Suzuki Y, Suzuki MG, Katsuma S. 2014. A single female-specific piRNA is the primary determiner of
785 sex in the silkworm. *Nature* 509:633–636. https://doi.org/10.1038/nature13315.
786 Kopp A. 2012. *Dmrt* genes in the development and evolution of sexual dimorphism. *Trends Genet* 28:175–
787 184. DOI: https://doi.org/10.1016/j.tig.2012.02.002.
788 Kunte K. 2008. Mimetic butterflies support Wallace's model of sexual dimorphism. *Proc R Soc B*
789 275:1617–1624. DOI: https://doi.org/10.1098/rspb.2008.0171.
790 Kuo TH, Fedina TY, Hansen I, Dreisewerd K, Dierick HA, Yew JY, Pletcher S.D. 2012. Insulin signaling
791 mediates sexual attractiveness in *Drosophila*. *PLoS Genet* 8:e1002684. DOI:
792 https://doi.org/10.1371/journal.pgen.1002684.
793 Lepage G, Roy C. 1984. Improved recovery of fatty acid through direct transesterification without prior
794 extraction or purification. *J Lipid Res* 25:1391–1396.
795 Legendre A, Miao XX, Da Lage JL, Wicker-Thomas C. 2008. Evolution of a desaturase involved in female
796 pheromonal cuticular hydrocarbon biosynthesis and courtship behavior in *Drosophila*. *Insect Biochem*
797 *Mol Biol* 38:244–255. DOI: https://doi.org/10.1016/j.ibmb.2007.11.005.
798 Li DT, Chen X, Wang XQ, Zhang CX. 2019a. *FAR* gene enables the brown planthopper to walk and jump
799 on water in paddy field. *Sci China Life Sci* 62:1521–1531. DOI: https://doi.org/10.1007/s11427-018-

800 9462-4.
801 Li DT, Chen X, Wang XQ, Moussian, B, Zhang CX. 2019b. The fatty acid elongase gene family in the
802 brown planthopper, *Nilaparvata lugens*. *Insect Biochem Mol Biol* 108:32–43. DOI:
803 https://doi.org/10.1016/j.ibmb.2019.03.005.
804 Livak KJ, Schmittgen TD, 2001. Analysis of relative gene expression data using real-time quantitative PCR
805 and the 2(-Delta Delta C(T)) method. *Methods* 25:402–408. DOI:
806 https://doi.org/10.1006/meth.2001.1262.
807 Lozano J, Belles X. 2011. Conserved repressive function of Krüppel homolog 1 on insect metamorphosis in
808 hemimetabolous and holometabolous species. *Sci Rep* 1:163. https://doi.org/10.1038/srep00163.
809 MacLean M, Nadeau J, Gurnea T, Tittiger C, Blomquist GJ. 2018. Mountain pine beetle (*Dendroctonus*
810 *ponderosae*) *CYP4Gs* convert long and short chain alcohols and aldehydes to hydrocarbons. *Insect*
811 *Biochem Mol Biol* 102:11–20. DOI: https://doi.org/10.1016/j.ibmb.2018.09.005.
812 Mank JE. 2017. The transcriptional architecture of phenotypic dimorphism. *Nature Ecol Evol* 1:6. DOI:
813 https://doi.org/10.1038/s41559-016-0006.
814 Marican C, Duportets L, Birman S, Jallon JM. 2004. Female-specific regulation of cuticular hydrocarbon
815 biosynthesis by dopamine in *Drosophila melanogaster*. *Insect Biochem Mol Biol* 34:823–830. DOI:
816 https://doi.org/10.1016/j.ibmb.2004.05.002.
817 Moon YA, Shah NA, Mohapatra S, Warrington JA, Horton JD. 2001. Identification of a mammalian long
818 chain fatty acyl elongase regulated by sterol regulatory element-binding proteins. *J Biol Chem*
819 276:45358–45366. DOI: https://doi.org/10.1074/jbc.M108413200.
820 Nojima S, Nishida R, Kuwahara Y, Sakuma M. 1999. Nuptial feeding stimulants: a male courtship
821 pheromone of the German cockroach, *Blattella germanica* (L.) (Dictyoptera: Blattellidae).
822 *Naturwissenschaften* 86:193-196. DOI: https://doi.org/10.1007/s001140050596.
823 Oh, CS, Toke DA, Mandala S, Martin CE. 1997. *ELO2* and *ELO3*, Homologues of the *Saccharomyces*
824 *cerevisiae ELO1* gene, function in fatty acid elongation and are required for sphingolipid formation. *J*
825 *Boil Chem* 272:17376–17384. DOI: https://doi.org/10.1074/jbc.272.28.17376.
826 Ohno Y, Suto S, Yamanaka M, Mizutani Y, Mitsutake S, Igarashi Y, Sassa T, Kihara A. 2010. ELOVL1
827 production of C24 acyl-CoAs is linked to C24 sphingolipid synthesis. *Proc Natl Acad Sci USA*
828 107:18439–18444. DOI: https://doi.org/10.1073/pnas.1005572107.

829 Parvy JP, Napal L, Rubin T, Poidevin M, Perrin L, Wicker-Thomas C, Montagne J. 2012. *Drosophila*
830 *melanogaster* Acetyl-CoA-carboxylase sustains a fatty acid-dependent remote signal to waterproof the
831 respiratory system. *PLoS Genets* 8:e1002925. DOI: https://doi.org/10.1371/journal.pgen.1002925.
832 Pei XJ, Chen N, Bai Y, Qiao JW, Li S, Fan YL, Liu TX. 2019. *BgFas1*: A fatty acid synthase gene required
833 for both hydrocarbon and cuticular fatty acid biosynthesis in the German cockroach, *Blattella*
834 *germanica* (L.). *Insect Biochem Mol Biol* 112:103203. DOI:
835 https://doi.org/10.1016/j.ibmb.2019.103203.
836 Pfannenstiel RS, Booth W, Vargo EL, Schal C. 2008. *Blattella asahinai* (Dictyoptera: Blattellidae): A new
837 predator of lepidopteran eggs in south Texas soybean. *Ann Entomol Soc Am* 101:763–768.
838 Prakash A, Monteiro A. 2016. Molecular mechanisms of secondary sexual trait development in insects.
839 *Curr Opin Insect Sci* 17:40–48. DOI: https://doi.org/10.1016/j.cois.2016.06.003.
840 Qiu Y, Tittiger C, Wicker-thomas C, Goff LG, Young S, Wajnberg E, Fricaux T, Taquet N, Blomquist GJ,
841 Feyereisen R. 2012. An insect-specific p450 oxidative decarbonylase for cuticular hydrocarbon
842 biosynthesis. *Proc Natl Acad Sci USA* 109:14858–14863. DOI:
843 https://doi.org/10.1073/pnas.1208650109.
844 Rogers TF, Palmer DH, Wright AE. 2020. Sex-specific selection drives the evolution of alternative splicing
845 in birds. *Mol Biol Evol*: In press. DOI: https://doi.org/10.1093/molbev/msaa242.
846 Romaá I, Pascual, N, X. Bellés. 1995. The ovary is a source of circulating ecdysteroids in *Blattella*
847 *germanica* (Dictyoptera: Blattellidae). *Eur J Entomol* 92:93-103.
848 Schal C, Burns EL, Jurenka RA, Blomquist GJ. 1990. A new component of the female sex pheromone of
849 *Blattella germanica* (L.) (Dictyoptera: Blattellidae) and interaction with other pheromone components.
850 *J Chem Ecol* 16:1997–2008. DOI: https://doi.org/10.1007/BF01020511.
851 Schal C, Gu X, Burns EL, Blomquist GJ. 1994. Patterns of biosynthesis and accumulation of hydrocarbons
852 and contact sex pheromone in the female German cockroach, *Blattella germanica*. *Arch Insect*
853 *Biochem Physiol* 25:375–391. DOI: https://doi.org/10.1002/arch.940250411.
854 Schal C, Chiang AS. 1995. Hormonal control of sexual receptivity in cockroaches. *Experientia* 51:994–
855 998. DOI: https://doi.org/10.1007/BF01921755.
856 Schal C, Sevala V, Cardé RT. 1998. Novel and highly specific transport of a volatile sex pheromone by
857 hemolymph lipophorin in moths. *Naturwissenschaften* 85: 339–342. DOI:

858 https://doi:10.1007/s001140050511.
859 Schal C, Sevala V, Capurro ML, Snyder TE, Blomquist GJ, Bagnères AG. 2001. Tissue distribution and
860 lipophorin transport of hydrocarbons and sex pheromones in the house fly, *Musca domestica*. *J Insect*
861 *Sci* 1:12.
862 Schal C. 2011. Cockroaches. In Hedges S, Moreland D, editors, Handbook of Pest Control, chapter 2, pages
863 150–291. Pennsylvania State University: GIEMedia.
864 Shirangi TR, Dufour HD, Williams TM, Carroll SB. 2009. Rapid evolution of sex pheromone-producing
865 enzyme expression in *Drosophila*. *PLoS Biol* 7:e1000168. DOI:
866 https://doi.org/10.1371/journal.pbio.1000168.
867 Tanaka K, Barmina O, Sanders LE, Arbeitman MN, Kopp A. 2011. Evolution of sex-specific traits through
868 changes in HOX-dependent *doublesex* expression. *PLoS Biol* 9:e1001131. DOI:
869 https://doi.org/10.1371/journal.pbio.1001131.
870 Toke DA, Martin CE. 1996. Isolation and characterization of gene affecting fatty acid elongation in
871 *Saccharomyces cerevisiae*. *J Biol Chem* 271:18413–18422. DOI:
872 https://doi.org/10.1074/jbc.271.31.18413.
873 Verhulst EC, van de Zande L.2015. Double nexus–*Doublesex* is the connecting element in sex
874 determination. *Brief Funct Genomics* 14:396–406. DOI: https://doi.org/10.1093/bfgp/elv005.
875 Wada-Katsumata A Schal, C. 2019. Antennal grooming facilitates courtship performance in a group-living
876 insect, the German cockroach *Blattella germanica*. *Sci Rep* 9:2942. DOI:
877 https://doi.org/10.1038/s41598-019-39868-x.
878 Wexler J, Delaney EK, Belles X, Schal C, Wada-Katsumata A, Amicucci MJ, Kopp A. 2019.
879 Hemimetabolous insects elucidate the origin of sexual development via alternative splicing. *eLife*
880 8:e47490. DOI: https://doi.org/10.7554/eLife.47490.
881 Wicker C, Jallon JM. 1995a. Hormonal control of sex pheromone biosynthesis in *Drosophila melanogaster*.
882 *J Insect Physiol* 41:65–70. DOI: https://doi.org/10.1016/0022-1910(94)00074-Q.
883 Wicker C, Jallon JM. 1995b. Influence of ovary and ecdysteroids on pheromone biosynthesis in *Drosophila*
884 *melanogaster* (Diptera: Drosophilidae). *Eur J Entomol* 92:197202.
885 Wicker-Thomas C, Garrido D, Bontonou G, Napal L, Mazuras N, Denis B. Rubin T, Parvy JP, Montagne J.
886 2015. Flexible origin of hydrocarbon/pheromone precursors in *Drosophila melanogaster*. *J Lipid Res*

887 56:2094–2101. DOI: https://doi.org/10.1194/jlr.M060368.

888 Williams TM, Selegue JE, Werner T, Gompel N, Kopp A, Carroll SB. 2008. The regulation and evolution
889 of a genetic switch controlling sexually dimorphic traits in *Drosophila*. *Cell* 134:610–623. DOI:
890 https://doi.org/10.1016/j.cell.2008.06.052.

891 Yew JY, Chung H. 2015. Insect pheromones: An overview of function, form, and discovery. *Prog Lipid Res*
892 59:88–105. DOI: https://doi.org/10.1016/j.plipres.2015.06.001.

893 Young HP, Larabee JK, Gibbs AG, Schal C. 2000. Relationship between tissue-specific hydrocarbon
894 profiles and lipid melting temperatures in the cockroach *Blattella germanica*. *J Chem Ecol* 26:1245-
895 1263. DOI: https://doi.org/10.1023/A:1005440212538.

896 Zhang Z, Klein J, Nei M. 2014a. Evolution of the *sex-lethal* gene in insects and origin of the sex-
897 determination system in *Drosophila*. *J Mol Evol* 78:50–65. DOI: https://doi.org/10.1007/s00239-013-
898 9599-3.

899 Zhang B, Xue HJ, Song KQ, Liu J, Li WZ, Nie RE, Yang XK. 2014b. Male mate recognition via cuticular
900 hydrocarbons facilitates sexual isolation between sympatric leaf beetle sister species. *J Insect Physiol*
901 70:15–21. DOI: https://doi.org/10.1016/j.jinsphys.2014.08.006.

902 Zhao X, Yang Y, Niu N, Zhao Y, Zhang J. 2020. The fatty acid elongase gene *LmElo7* is required for
903 hydrocarbon biosynthesis and cuticle permeability in the migratory locust, *Locusta migratoria*. *J*
904 *Insect Physiol* 123: 104052. DOI: https://doi.org/10.1016/j.jinsphys.2020.104052.

905 Zinna RA, Gotoh H, Kojima T, Niimi T. 2018. Recent advances in understanding the mechanisms of
906 sexually dimorphic plasticity: insights from beetle weapons and future directions. *Curr Opin Insect Sci*
907 25:35–41. DOI: https://doi.org/10.1016/j.cois.2017.11.009.

908

Figures and figure legends

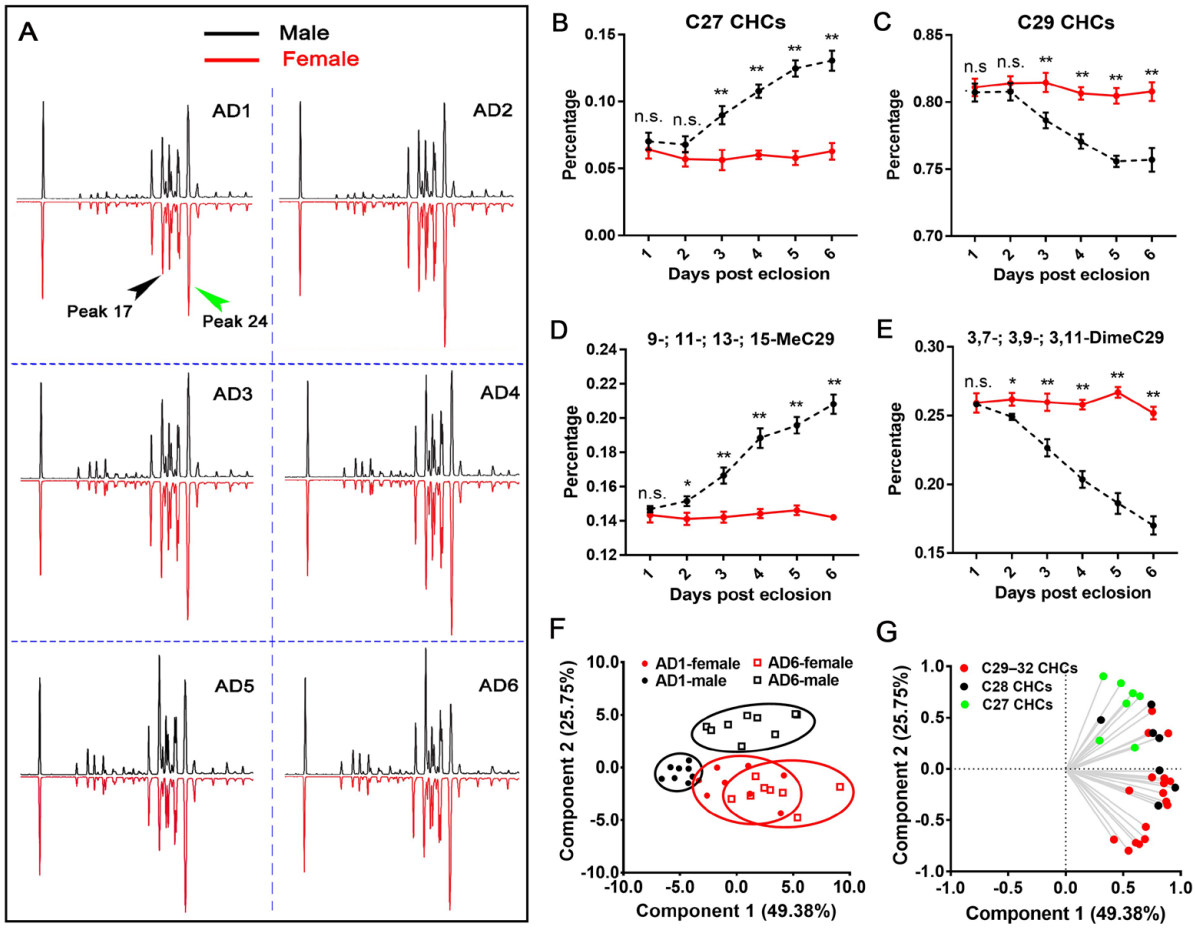

Figure 1. Development of sexually dimorphic cuticular hydrocarbons. **(A)** Comparisons of 1- to 6-day-old adult (AD1–AD6) male (black) and female (red) cuticular hydrocarbon profiles. The first peak represents the internal standard *n*-hexacosane. Other peaks correspond to the CHCs in Source data 1. Peak 17 is male-enriched (9-; 11-; 13-; 15-MeC29) and gradually increased with age in males. Peak 24 is female-enriched (3,7-; 3,9-; 3,11-DimeC29). The proportions of C27 CHCs **(B)**, C29 CHCs **(C)**, Peak 17 **(D)**, and Peak 24 **(E)** in the total CHCs from AD1 to AD6 were compared between males (black dashed lines) and females (solid red lines). Data are shown as mean ± SEM (n.s. represents no significant difference; $*P < 0.05$, $**P < 0.01$, two-tailed Student's *t*-test, n = 8–10). **(F, G)** Principal component analysis of AD1 and AD6 CHC profiles of males and females. In **(F)**, each dot represents a datum calculated from one cockroach. AD1 male (black solid circles) and female (red solid circles) CHC profiles overlapped, whereas AD6 male (black open square) and female (red open square) CHC profiles separated along PC2. In the loading diagram **(G)**, CHCs with different chain lengths are marked by green (C27), black (C28), and red (C29–C32), showing that C27 CHCs vectored toward males along PC2, whereas longer chain CHCs vectored toward females.

925 The following Source data and Figure supplements are available for Figure 1:

926 **Source data 1.** Quantification of different cuticular hydrocarbons during sexually dimorphic cuticular

927 hydrocarbon generation.

928 **Figure 1–figure supplement 1.** Cuticular hydrocarbon profiles of 4-day-old sixth-instar nymphs of *Blattella*

929 *germanica*.

930

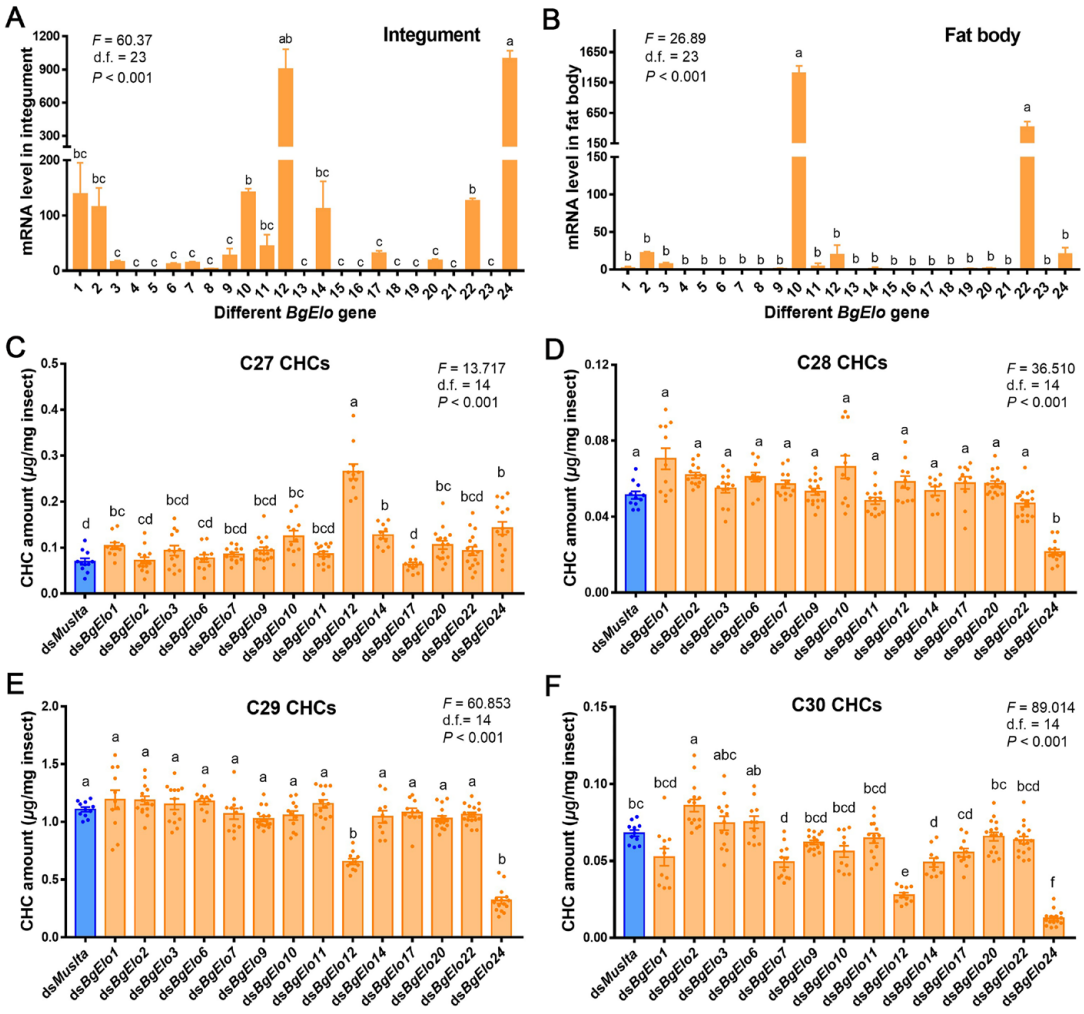

Figure 2. RNAi screen to identify *BgElo* genes involved in long-chain cuticular hydrocarbon biosynthesis. Transcript levels of different *BgElo* genes in the abdominal integument **(A)** and fat body **(B)**. The numbers on the abscissa correspond to *BgElo1–24*. Data are shown as mean ± SEM, and calculated from 4 replicates (each replicate contains 4 cockroaches for the integument and 8 cockroaches for the fat body). The influence of knockdown of different *BgElo* genes on C27 **(C)**, C28 **(D)**, C29 **(E)**, and C30 **(F)** CHCs is shown. Data are presented as mean ± SEM and calculated from 10–16 AD2 female cockroaches, each dot indicating a single datum from one cockroach. Only RNAi of *BgElo12* and *BgElo24* resulted in significant increases of C27 CHCs and decreases of C29 CHCs. Different letters indicate statistically significant differences between groups using Welch's ANOVA (Games-Howell multiple comparisons test, $P < 0.05$).

The following Source data and Figure supplements are available for Figure 2:

Source data 2. Quantification of individual cuticular hydrocarbons after RNAi of *BgElo* genes.

Figure 2–figure supplement 1. RNAi efficiency of different *BgElo* genes in *Blattella germanica*.

945 **Figure 2–figure supplement 2.** Influence of *BgElo*-RNAi on cuticular hydrocarbons with chain length longer

946 than 30 carbons.

947

948

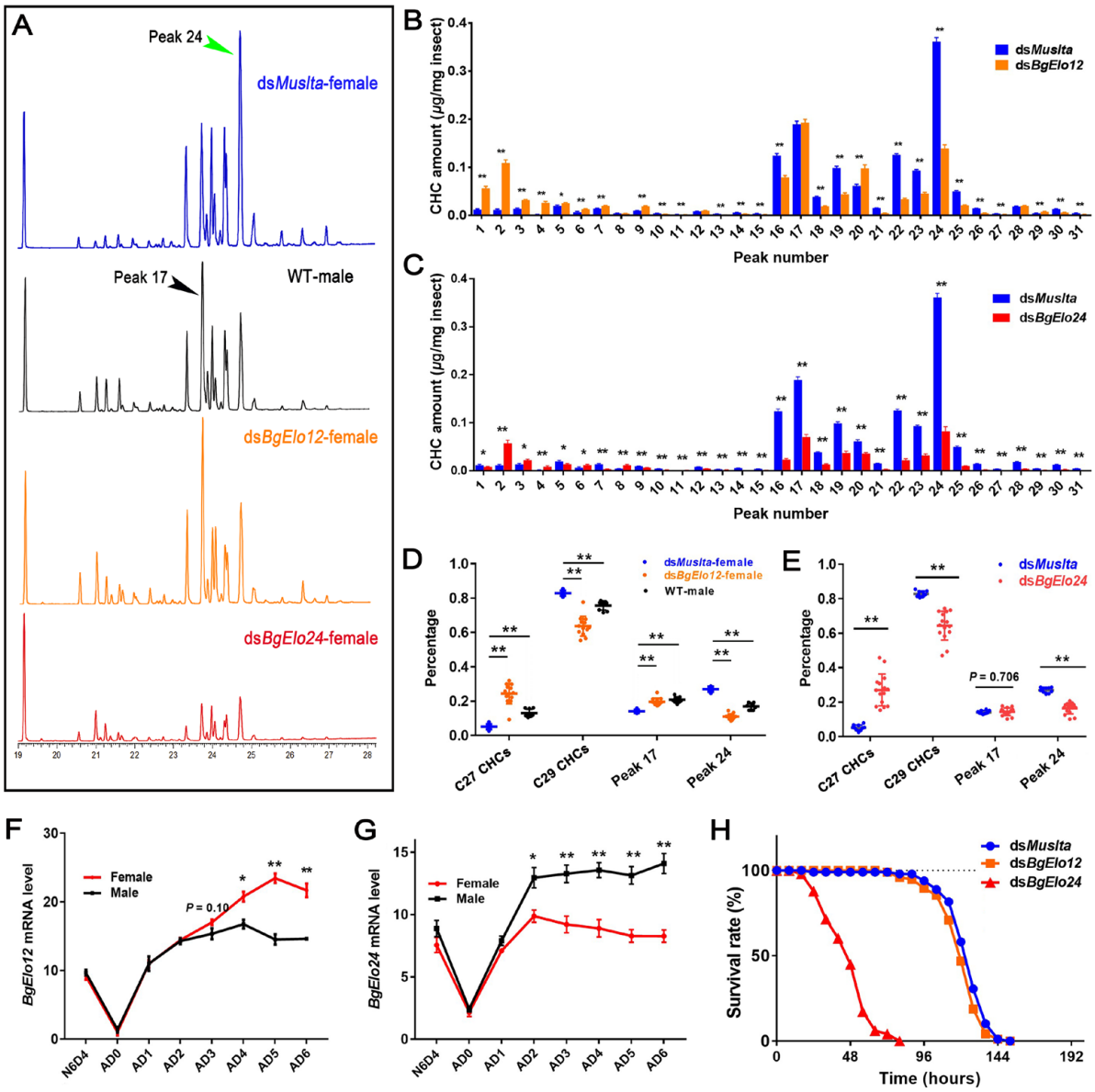

Figure 3. *BgElo12* is involved in generating sexually dimorphic hydrocarbons. **(A)** Gas chromatogram of CHC profiles from differently treated cockroaches. The CHC profiles of sexually mature females and males (AD6–AD8) showed a marked difference, and RNAi of only *BgElo12* in females generated a male-like CHC profile. Quantitative influence of *BgElo12*-RNAi **(B)** and *BgElo24*-RNAi **(C)** in females on the amount of each CHC. Percentage change of the C27 CHCs, C29 CHCs, male-enriched peak 17, and female-enriched peak 24 after *BgElo12*-RNAi **(D)** or *BgElo24*-RNAi **(E)**. Data in **(B–E)** are shown as mean ± SEM, *$P < 0.05$, **$P < 0.01$; two-tailed Student's *t*-test, n = 10 for *dsMuslta*, 11 for *dsBgElo12*, and 15 for *dsBgElo24*, 9 for wild type males (WT-male). Relative expression of *BgElo12* **(F)** and *BgElo24* **(G)** among different developmental stages and different ages of adult males and females. *P* values were calculated from 4 replicates (2–3 cockroaches/replicate), **$P < 0.01$; two-tailed Student's *t*-test. **(H)** Survival rates of *dsMuslta* (n = 98),

960 *dsBgElo12* (n = 96), and *dsBgElo24* (n = 98) treated female cockroaches maintained at 5% RH. Survival rates
961 were calculated every 8 h until all cockroaches died.
962
963 The following Figure supplements are available for Figure 3:
964 **Figure 3–figure supplement.** Influence of *BgElo12*-RNAi and *BgElo24*-RNAi on CHC profiles of male *B.*
965 *germanica*.
966 **Figure 3–figure supplement 2.** Verifying the influences of *BgElo12* and *BgElo24* on hydrocarbon biosynthesis
967 by using the second RNAi targets and examining changes of internal hydrocarbons.
968 **Figure 3–figure supplement 3.** Tissue-specific expression of *BgElo12* and *BgElo24*.
969
970

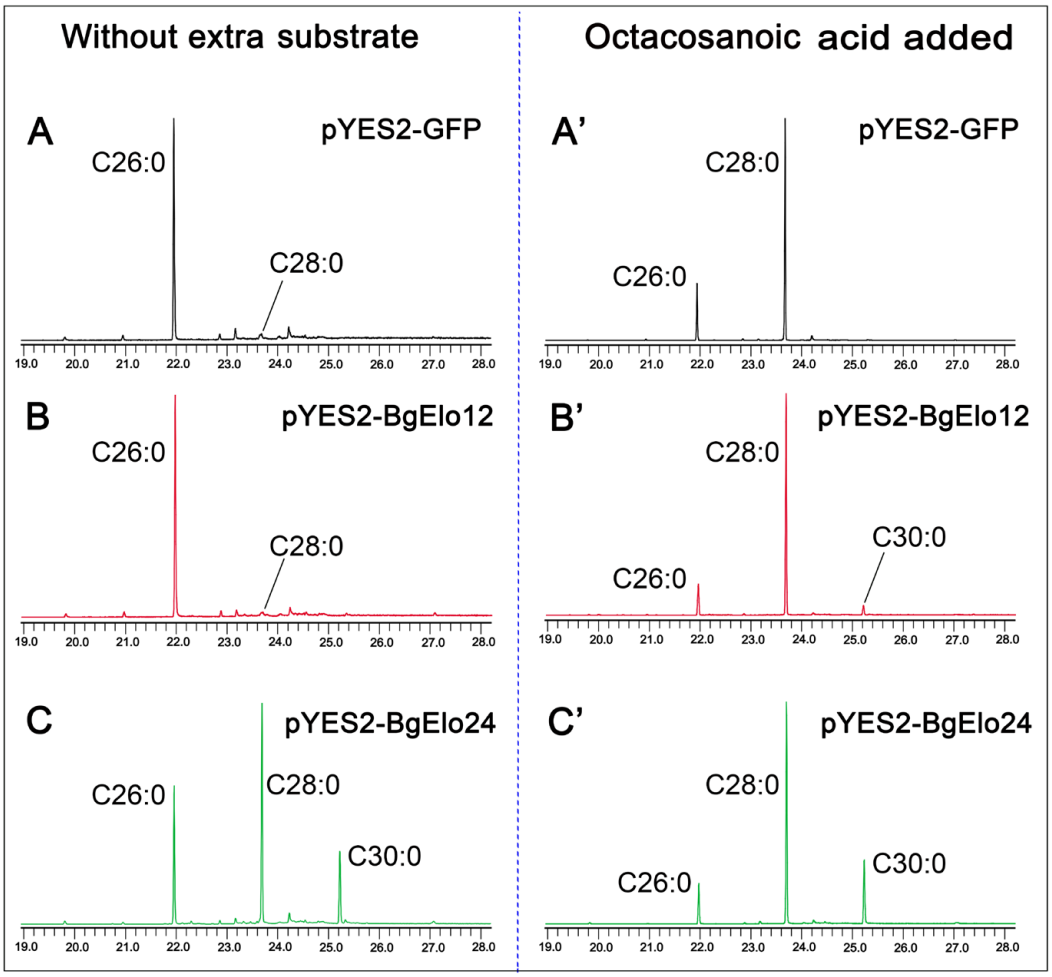

Figure 4. Yeast expression and substrate catalysis of BgElo12 and BgElo24. Representative gas chromatogram of fatty acid methyl esters of yeast transformed with pYES2-GFP **(A)**, pYES2-BgElo12 **(B)**, and pYES2-BgElo24 **(C)** without addition of extra substrates. After adding octacosanoic acid (C28:0), the corresponding chromatograms are shown at the right for pYES2-GFP **(A')**, pYES2-BgElo12 **(B')**, and pYES2-BgElo24 **(C')**. The chromatograms are truncated, and only chromatographic peaks of interest are indicated. The FAMEs are labeled by their corresponding saturated FAs. Complete chromatograms are shown in Figure 4–supplement figure 1.

The following source data and Figure supplements are available for Figure 4:

Source data 3. Calculation of the proportions of different fatty acid methyl esters in the yeast expression.

Figure 4–figure supplement 1. Heterologous expression of BgElo12 and BgElo24 with methyl-branched substrates.

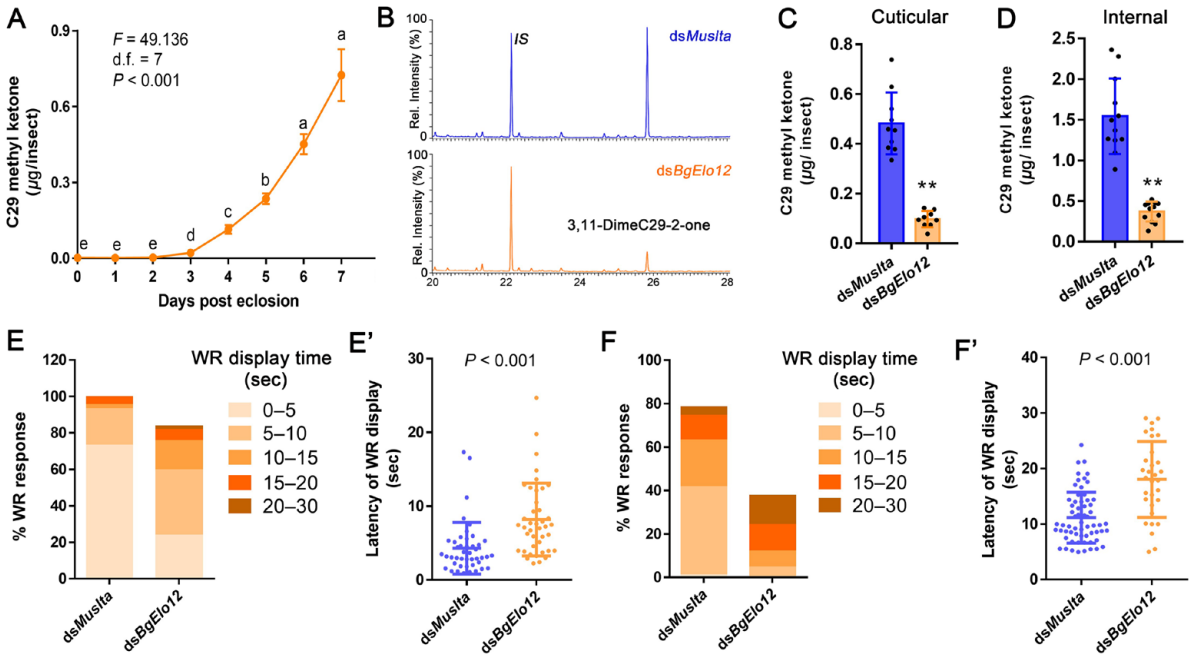

Figure 5. *BgElo12*-RNAi effects on contact sex pheromone biosynthesis in females and male courtship performance. **(A)** The pattern of contact sex pheromone (3,11-DimeC29-2-one) accumulation during female sexual maturation. Data are shown as mean ± SEM. Different letters indicate significant differences between groups using Welch's ANOVA (Games-Howell multiple comparisons test, $P < 0.05$). **(B)** Representative chromatogram showing lower amounts of sex pheromone after *BgElo12*-RNAi. *IS* is the internal standard 14-heptacosanone. Cuticular **(C)** and internal **(D)** amounts of 3,11-DimeC29-2-one (C29 methyl ketone) after *BgElo12*-RNAi. Data are shown as mean ± SD, and each replicate is shown as a dot. $^{**}P < 0.01$, two-tailed Student's *t*-test; n = 9–12. Influence of *BgElo12*-RNAi on the ability of AD5 **(E–E')** and AD3 **(F–F')** female antennae to elicit courtship in males. The percentage of males that responded with a wing-raising (WR) behavior in response to contact with female antenna were determined for 44 (*dsMuslta*) and 49 (ds*BgElo12*) female antennae in **(E)**, and 79 (ds*Muslta*) and 82 (ds*BgElo12*) antennae in **(F)**. Each female antenna was tested only once with a single male. The proportion of WR display over different time periods (latency, sec) is shown in progressively darker colors. **(E')** and **(F')** Average latency of WR display calculated from those antennae that successfully activated a courtship behavior of males within 30 s. Data are shown as mean ± SD, each dot represents a datum calculated from one antenna. *P* values were determined by two-tailed Student's *t*-test.

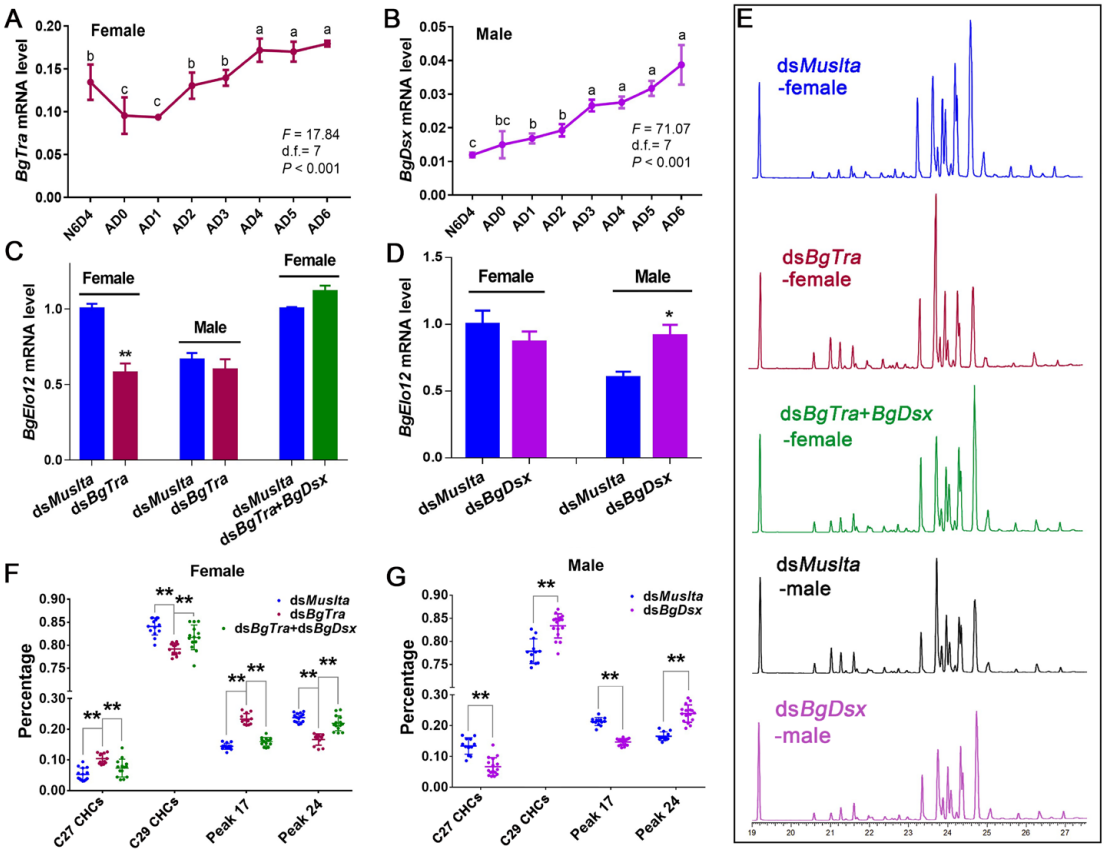

Figure 6. Regulation of *BgElo12* and sexually dimorphic hydrocarbon profiles by sex-differentiation genes. Temporal patterns of *BgTra* expression in females **(A)** and *BgDsx* expression in males **(B)**. Data are shown as mean ± SEM and calculated from 4 replicates (2–3 cockroaches/replicate). N6D4 is 6th instar nymph on day 4, AD0–6 represent adult days 0 to 6. Different letters indicate significant differences between the groups (ANOVA, Fisher's LSD, $P < 0.05$). **(C)** and **(D)** Regulation of *BgElo12* expression by *BgTra* and *BgDsx*. Data are shown as mean calculated from 4 replicates (2–3 cockroaches/replicate) ± SEM; *$P < 0.05$, **$P < 0.01$, two-tailed Student's *t*-test. **(E)** Gas chromatograms of CHCs after repressing different sex-differentiation genes. **(F)** Regulation of the proportions of representative CHCs by *BgTra* in females. Data are presented as mean ± SD, **$P < 0.01$; two-tailed Student's *t*-test; n = 14 for *dsMuslta*, 12 for ds*BgTra*, and 14 for ds*BgTra*+ds*BgDsx*. **(G)** The proportion change of representative CHCs after *BgDsx*-RNAi in males. Data are shown as mean ± SD; **$P < 0.01$; two-tailed Student's *t*-test, n = 12 for *dsMuslta* and 16 for ds*BgDsx*.

The following Figure supplements are available for Figure 6:

Figure 6–figure supplement 1. Verifying the sex-specific developmental function of *BgTra* and *BgDsx*.

Figure 6–figure supplement 2. Transcriptional activity of *BgDsx*^{M} on the upstream regulatory sequence of *BgElo12*.

1019 **Figure 6–figure supplement 3.** Influence of *BgDsx*-RNAi and *BgTra*-RNAi on *BgElo24* expression.

1020 **Figure 6–figure supplement 4.** Regulation of cuticular hrdrocarbon profiles by sex-differentiation genes.

1021 **Figure 6–figure supplement 5.** Regulation of internal hydrocarbon profiles by sex-differentiation genes.

1022 **Figure 6–figure supplement 6.** Regulation of *Krh1* by *BgTra* in females.

1023
1024

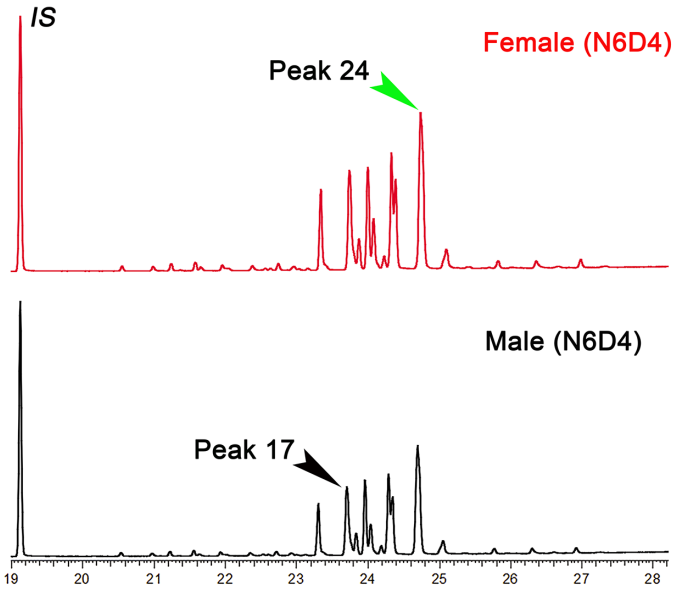

Figure 1–figure supplement 1. Cuticular hydrocarbon profiles of 4-day-old sixth-instar nymphs of *Blattella germanica*. Peak 24 represents the female-enriched 3,7-; 3,9-; 3,11-DimeC29, and Peak 17 is the male-enriched 9-; 11-; 13-; 15-MeC29.

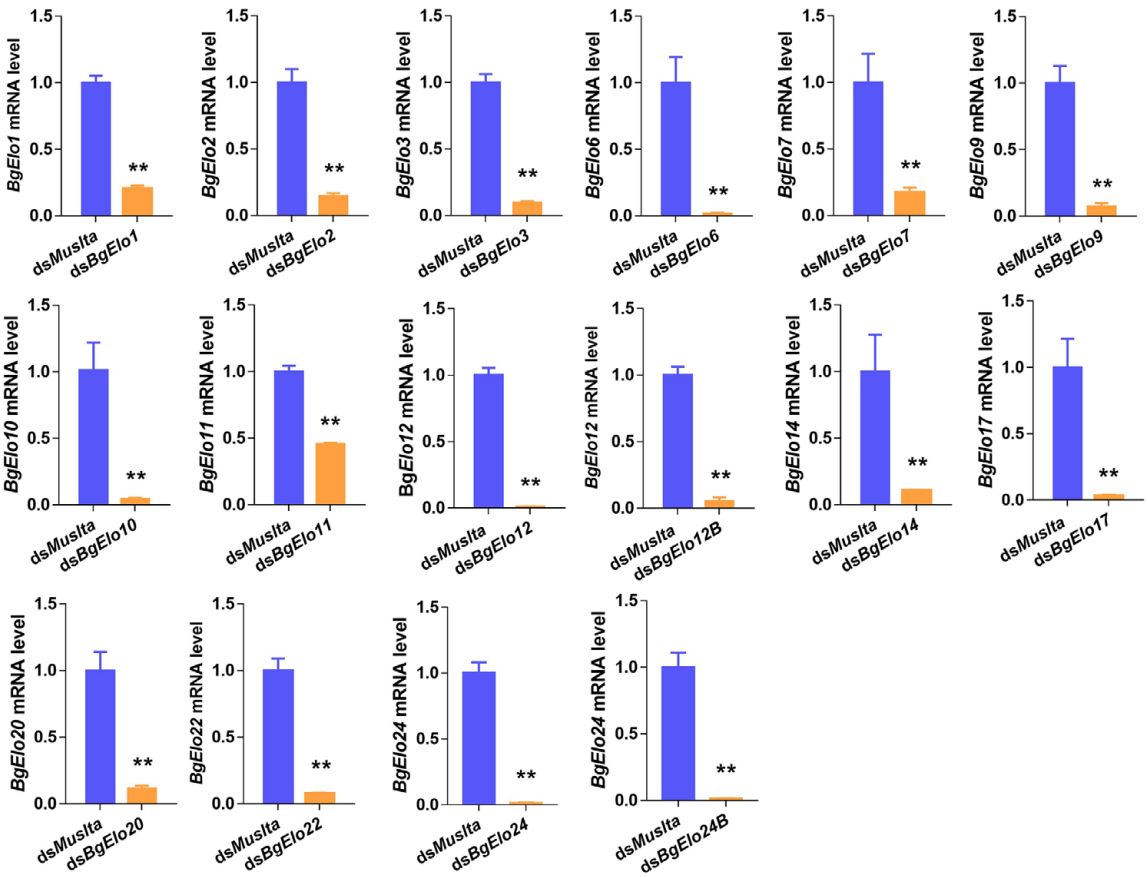

Figure 2–figure supplement 1. RNAi efficiency of different *BgElo* genes in *Blattella germanica*. Data are shown as mean ± SEM, calculated from 4 replicates (2–3 cockroaches/replicate); $^{**}P < 0.01$, two-tailed Student's *t*-test.

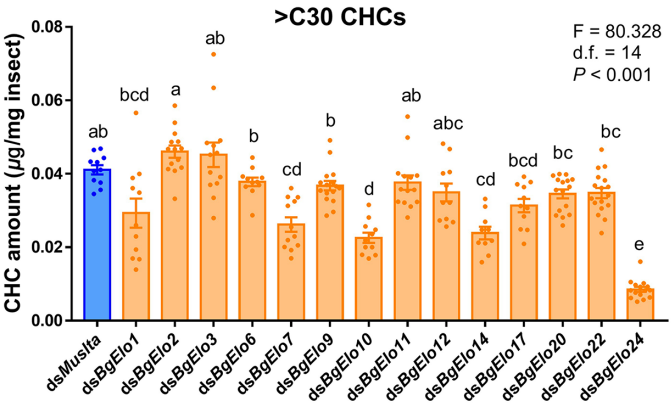

Figure 2–figure supplement 2. Effects of *BgElo*-RNAi on cuticular hydrocarbons of *Blattella germanica* with chain length longer than 30. Different letters indicate significant differences between groups using Welch's ANOVA (Games-Howell multiple comparisons test, $P < 0.05$).

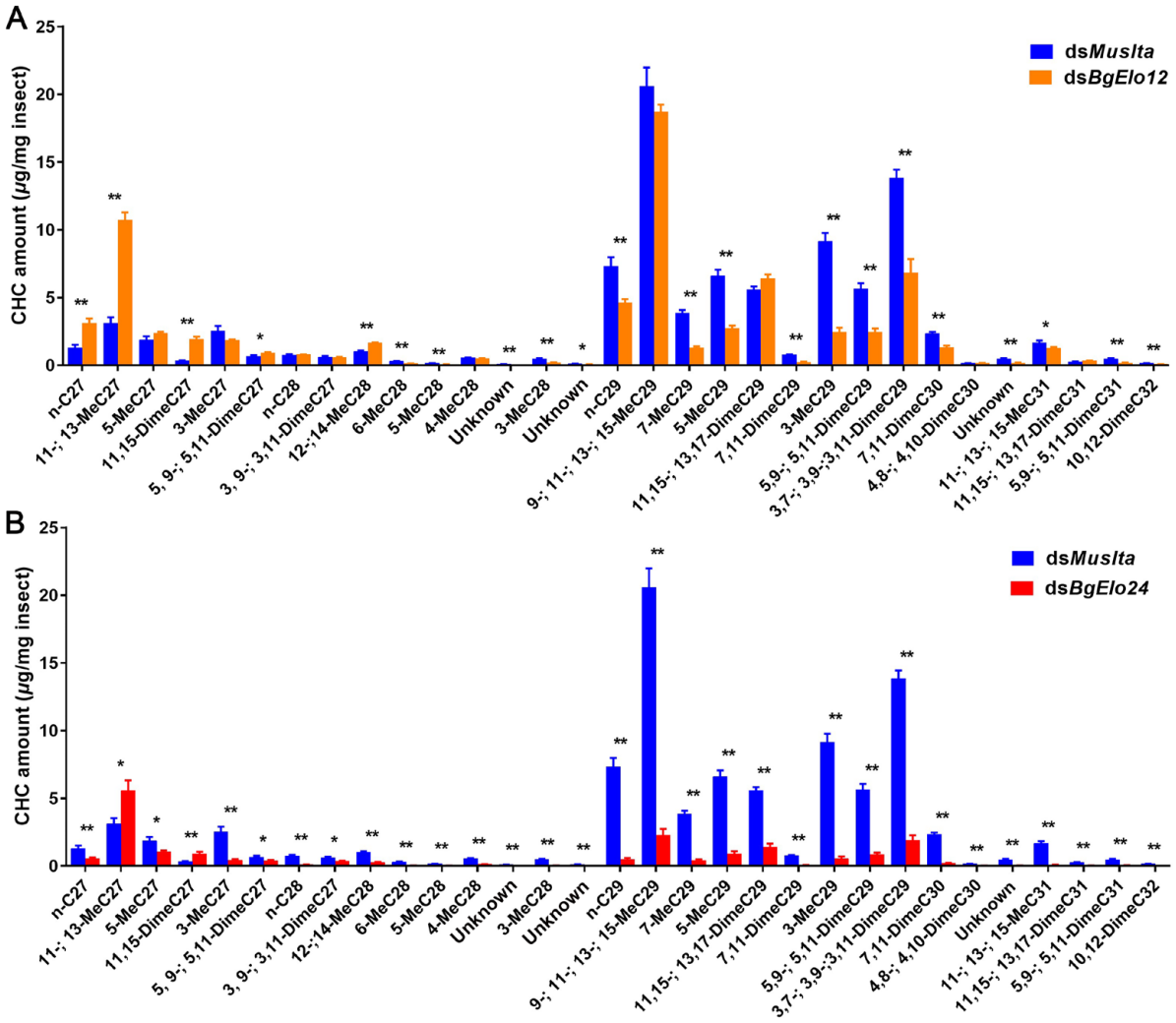

Figure 3–figure supplement 1. Effects of *BgElo12*-RNAi and *BgElo24*-RNAi on CHC profiles of male *B. germanica*. Data are shown as mean ± SEM; **P* < 0.05, ***P* < 0.01; two-tailed Student's *t*-test, n = 9 or 10.

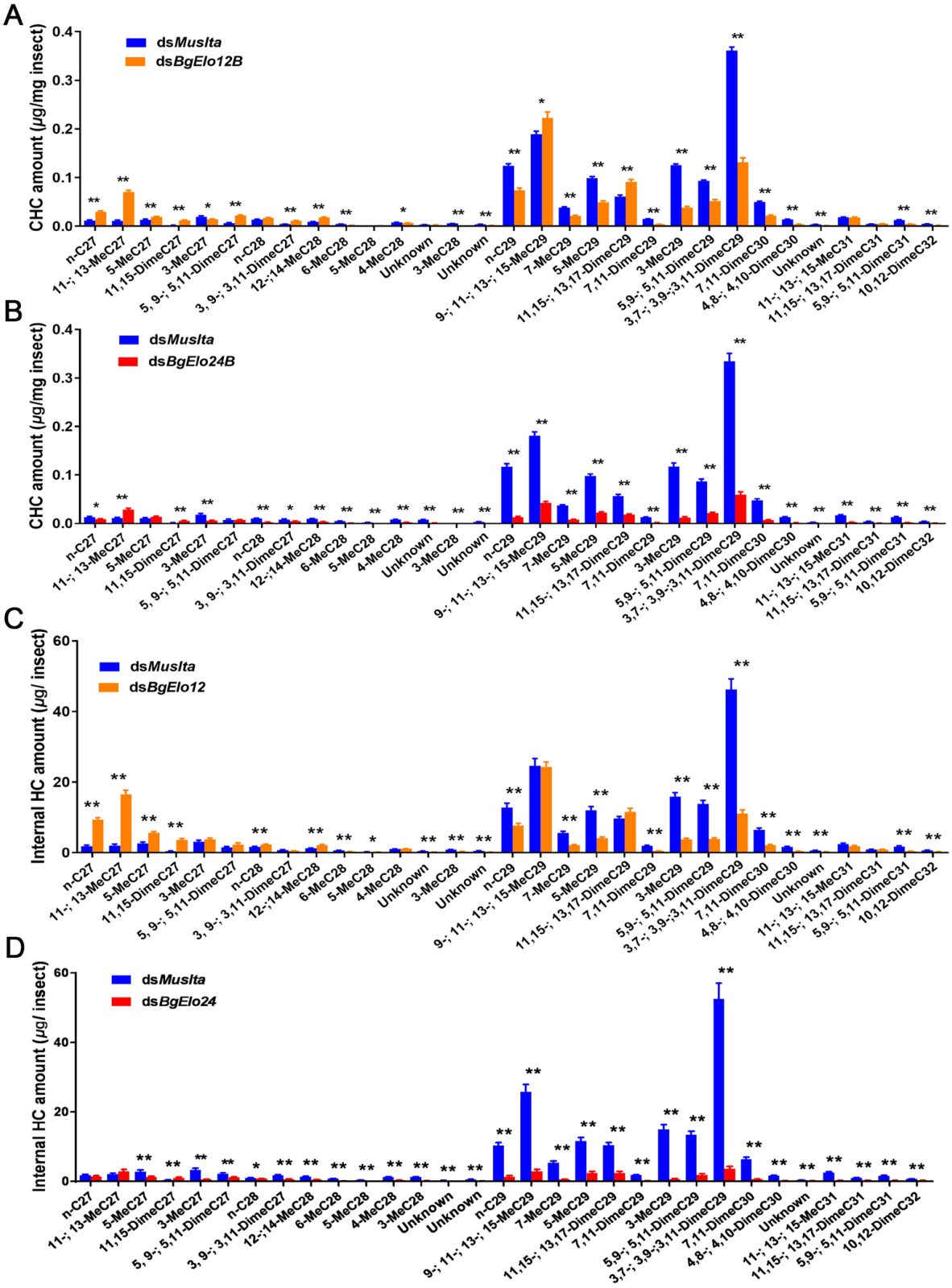

Figure 3–figure supplement 2. Verifying the roles of *BgElo12* and *BgElo24* in hydrocarbon biosynthesis by the second RNAi targets. **(A)** Analysis of cuticular hydrocarbons after RNAi of *BgElo12* using the second target (ds*BgElo12B*), **(B)** or after RNAi of *BgElo24* using the second target (ds*BgElo24B*). **(C)** and **(D)** The effects of

1047 *BgElo12*-RNAi and *BgElo24*-RNAi on internal hydrocarbons. Data are shown as mean ± SEM; *$P < 0.05$, **$P <$

1048 0.01; two-tailed Student's *t*-test, n = 10–12.

1049

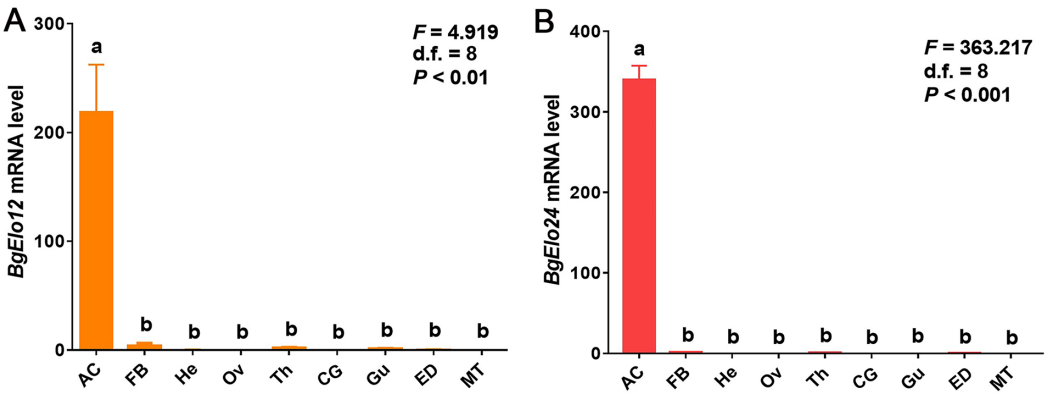

Figure 3–figure supplement 3. Tissue-specific expression of *BgElo12* and *BgElo24* in *Blattella germanica*. AC: Abdominal cuticle, FB: Fat body, He: Head, Ov: Ovaries, Th: Thorax, Cg: Colleterial gland, Gu: Gut, ED: Ejaculatory duct, MT: Malpighian tubules. Data are shown as mean ± SEM; and each sample was collected from 4 (AC, Th, Gu), 8 (FB, He, Ov, CG, ED), and 12 (MT) cockroaches. Different letters indicate significant differences between groups using Welch's ANOVA (Games-Howell multiple comparisons test, $P < 0.05$), n = 4.

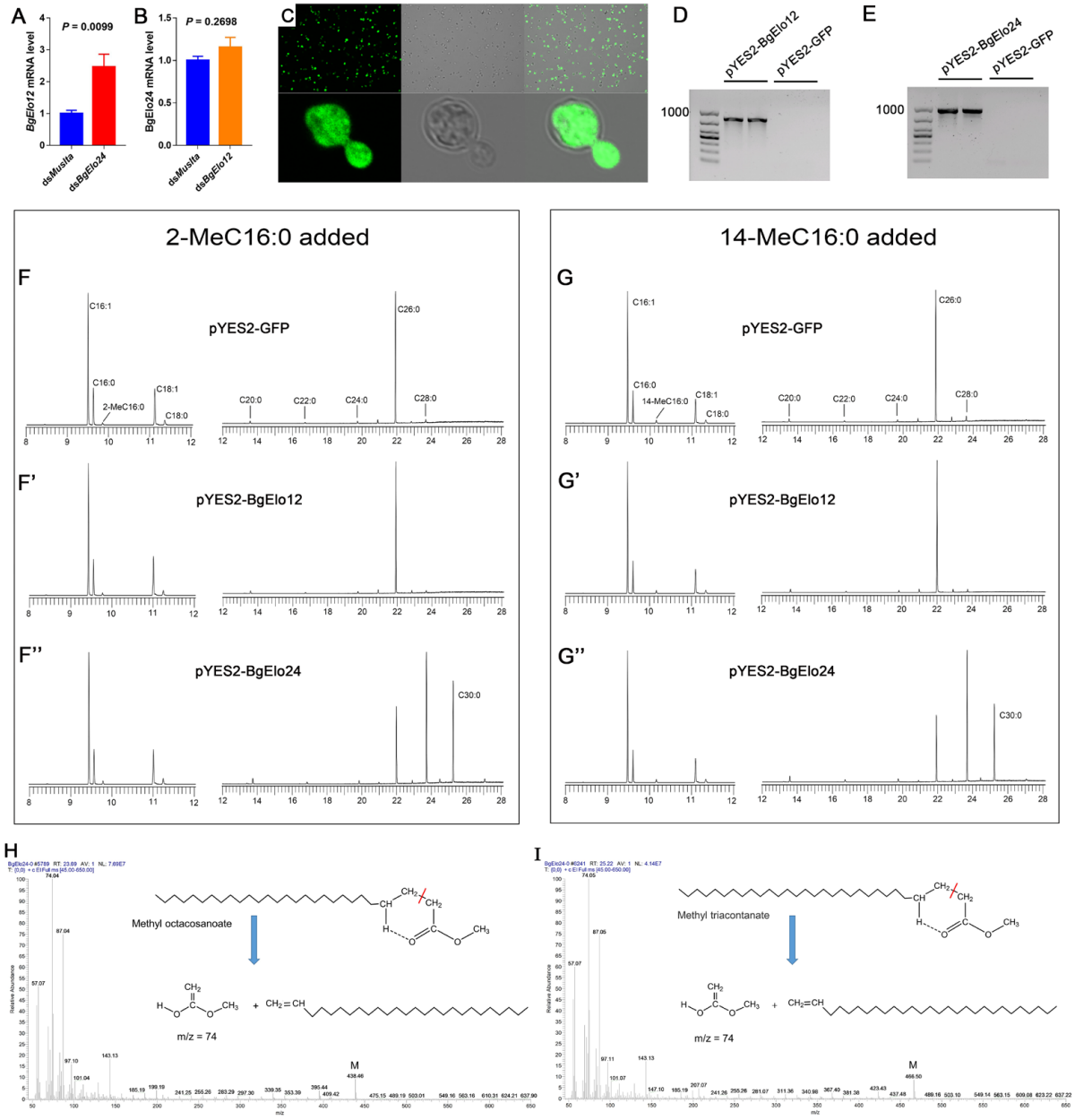

Figure 4–figure supplement 1. Heterologous expression of *BgElo12* and *BgElo24* in yeast. RNAi of *BgElo24* upregulated the expression of *BgElo12* **(A)**, while RNAi of *BgElo12* did not affect *BgElo24* transcript level **(B)**. Data are shown as mean ± SEM; *P* values were calculated from 4 samples; each sample contained 2 cockroaches; two-tailed Student's *t*-test. **(C)** Detection of GFP protein in the yeast with pYES2-GFP using a FV3000 confocal fluorescence microscope (Olympus). **(D)** and **(E)** RT-PCR analysis of the *BgElo12* and *BgElo24* mRNA after the induction with galactose. **(F)**, **(F')**, and **(F'')** Gas chromatograms of fatty acid methyl esters after adding 2-MeC16:0 into the medium. **(G)**, **(G')**, and **(G'')** Gas chromatogram of fatty acid methyl esters after adding 14-MeC16:0 into the medium. The compositions with retention times between 12 and 28 min

1066 were magnified about 50 times. **(H)** and **(I)** Mass spectra of methyl octacosanoate and methyl triacontanate, both

1067 of which showed a strong characteristic ion fragment (m/z = 74) and M peak.

1068

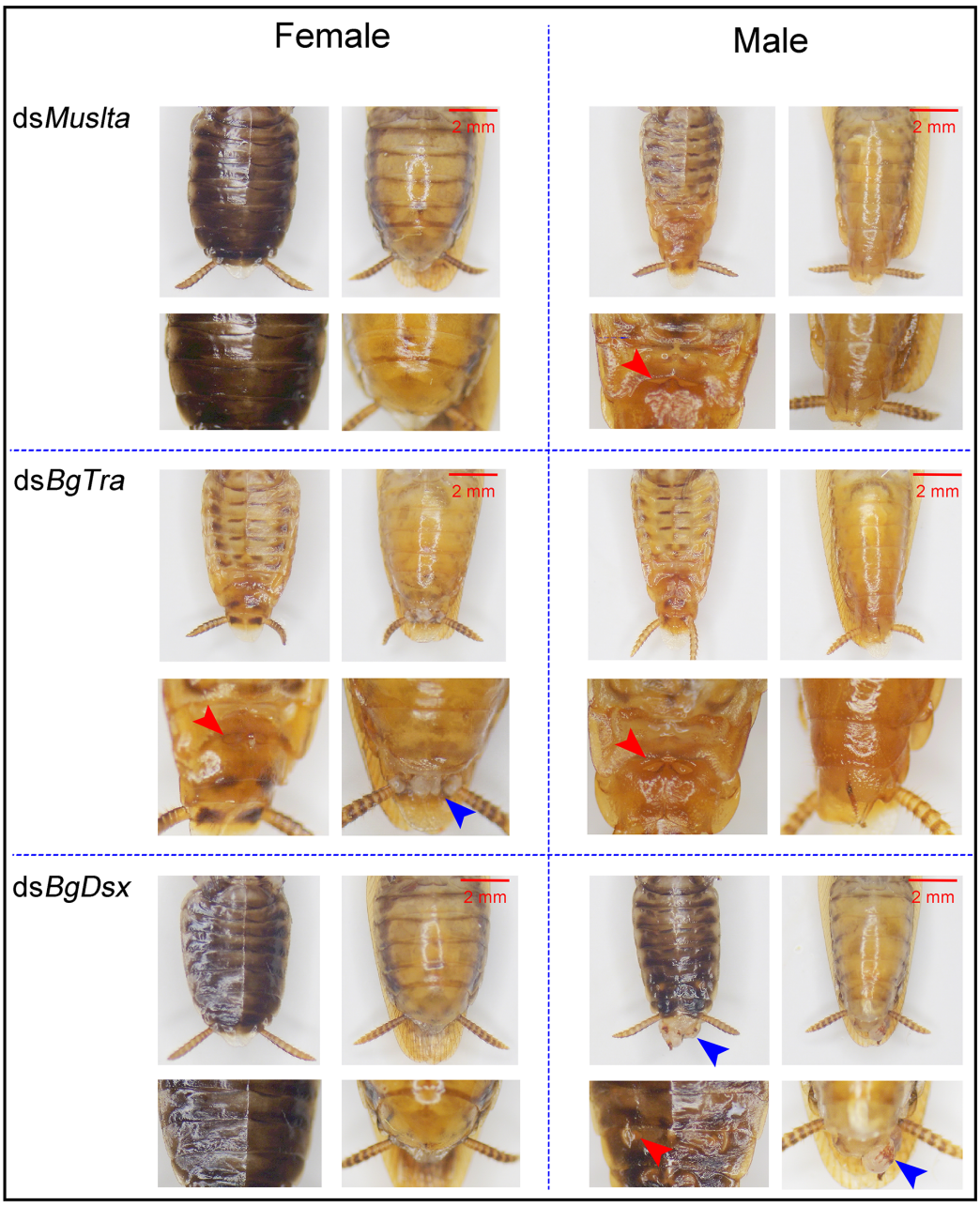

Figure 6–figure supplement 1. The sex-specific developmental functions of *BgTra* and *BgDsx* in *Blattella germanica*. RNAi of *BgTra* in females generated a male-like body size and cuticle color, male-like tergal gland structure and a protruding tissue at the end of the abdomen (left center); RNAi of *BgDsx* in males generated a female-like body color and a protruding tissue at the end of the abdomen, and the tergal gland partly disappeared (right bottom). Other treatments did not generate obvious developmental effects.

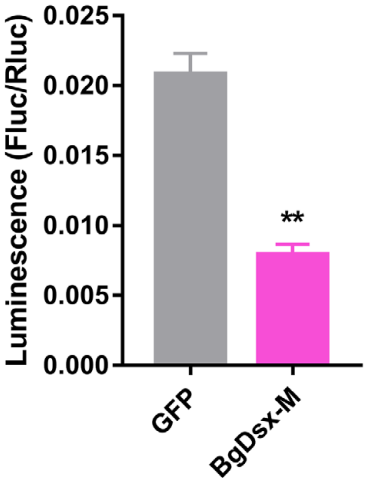

1076

1077 **Figure 6-figure supplentment 2.** Transcriptional activity of *BgDsx*^{M} on the upstream regulatory sequence of

1078 *BgElo12*. Data are shown as mean ± SEM; *P* values were calculated from 12 replicates; two-tailed Student's *t*-

1079 test.

1080

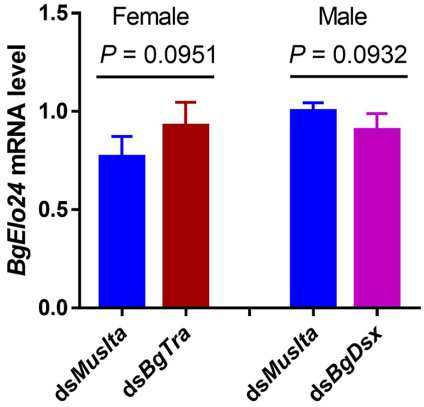

Figure 6–figure supplement 3. Effects of *BgDsx*-RNAi in males and *BgTra*-RNAi in females on *BgElo24* expression. Data are shown as mean ± SEM; *P* values were calculated from 4 replicates (2 cockroaches/replicate); two-tailed Student's *t*-test.

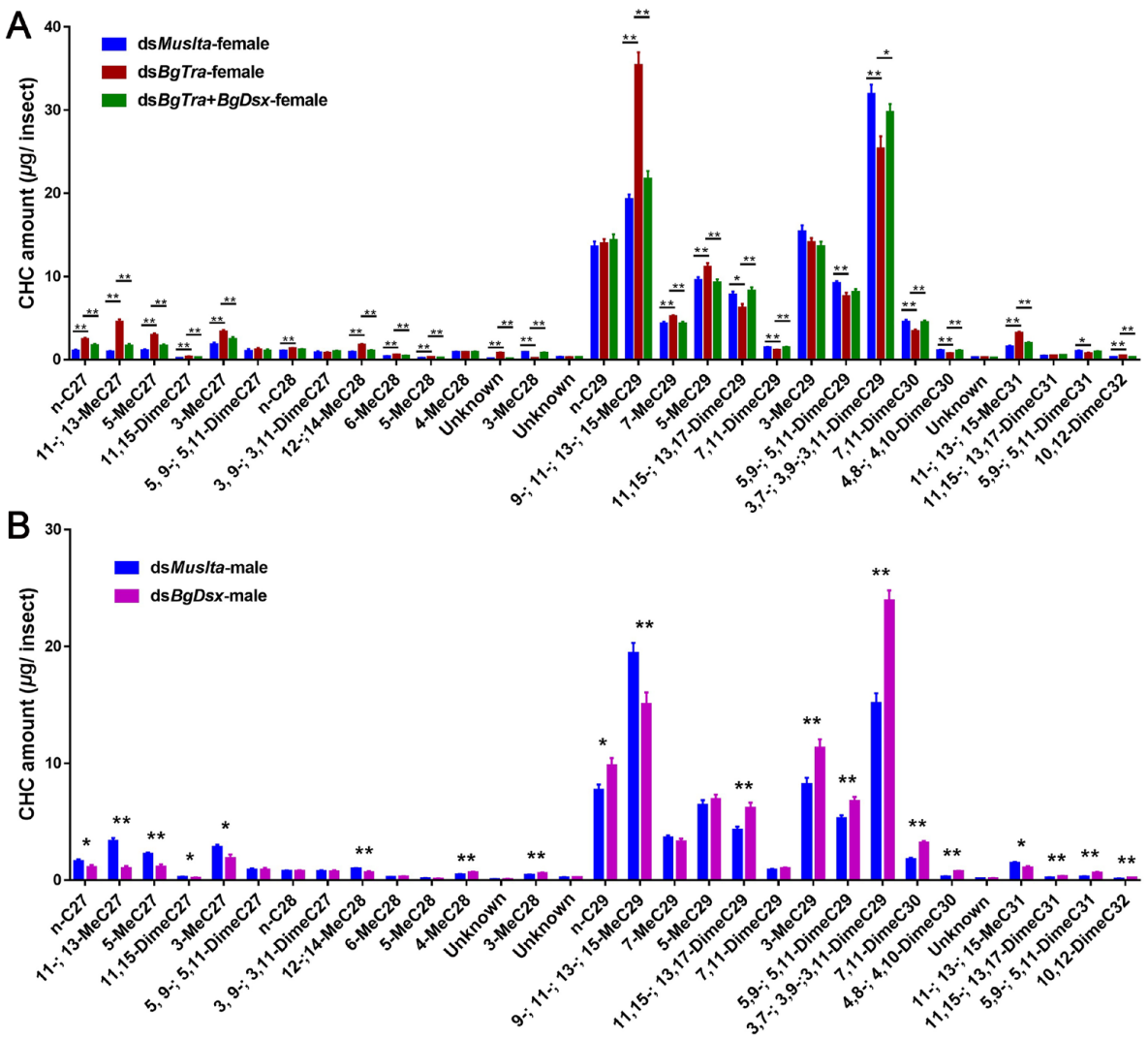

Figure 6–figure supplement 4. Regulation of cuticular hrdrocarbon profiles by sex-differentiation genes. Data are shown as mean ± SEM, **P* < 0.05, ***P* < 0.01, two-tailed Student's *t*-test, n = 14 (ds*Muslta*-female), 12 (ds*BgTra*-female), 14 (ds*BgTra*+ds*BgDsx*-female), 12 (ds*Muslta*-male), and 16 (ds*BgDsx*-male).

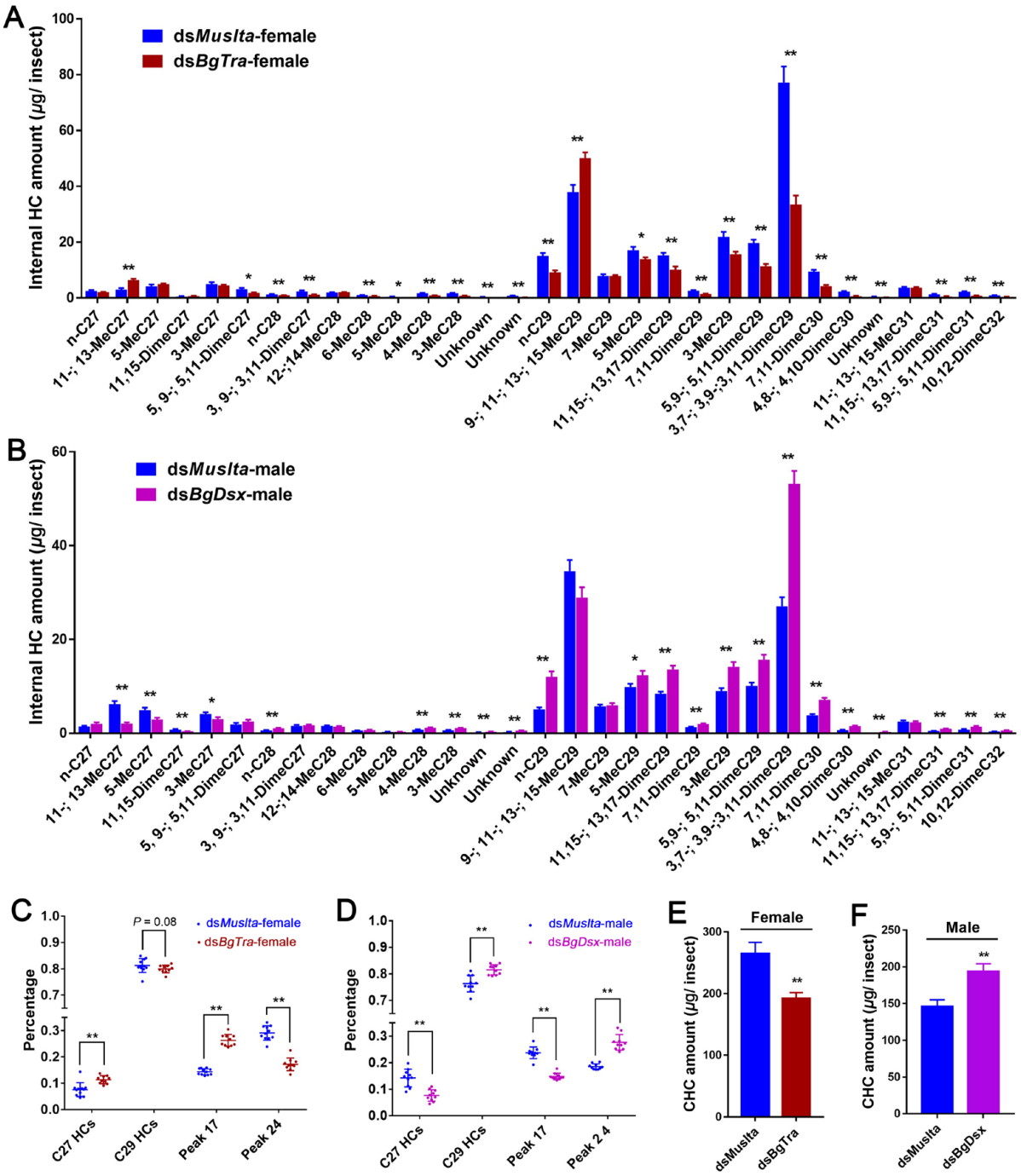

Figure 6–figure supplement 5. Regulation of internal hrdrocarbon profiles by sex-differentiation genes. **(A)** and **(B)** Effects of *BgTra*-RNAi in females and *BgDsx*-RNAi in males on sex-specific internal hydrocarbon profiles. **(C)** and **(D)** Proportion changes of representative internal hydrocarbons after RNAi of *BgTra* in females and *BgDsx* in males. **(E)** and **(F)** Effects of *BgTra*-RNAi in females and *BgDsx*-RNAi in males on total amounts of internal hydrocarbons. Data are shown as mean ± SEM, **P* < 0.05, ***P* < 0.01, two-tailed Student's *t*-test, n = 10 or 11.

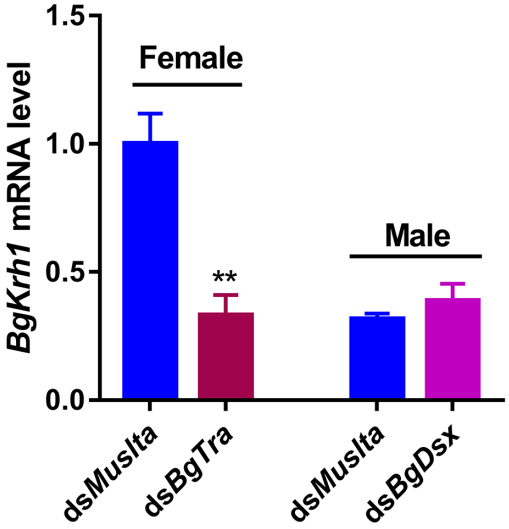

Figure 6–figure supplement 6. Regulation of *BgKrh1* by *BgTra* in females. Data are shown as mean ± SEM, *P* values were calculated from 4 replicates (2 cockroaches/replicate), $^{**}P < 0.01$, two-tailed Student's *t*-test.